



New Mechanistic Models of Creep-Fatigue Interactions for Gas Turbine Components (DE-FE0011796)

Thomas Siegmund

School of Mechanical Engineering, Purdue University

Email: siegmund@purdue.edu

Vikas Tomar

School of Aerospace and Aeronautical Engineering, Purdue University

Jamie Kruzic

Oregon State University (now University of New South Wales)



TEAM AND COLLABORATION

Purdue University

- Thomas Siegmund with Dr. Trung Nguyen (post doc)
- Vikas Tomar with Devendra Verma (PhD student)

Oregon State University

- Jay Kruzic with Halsey Ostergaard (PhD Student)

NETL Collaboration

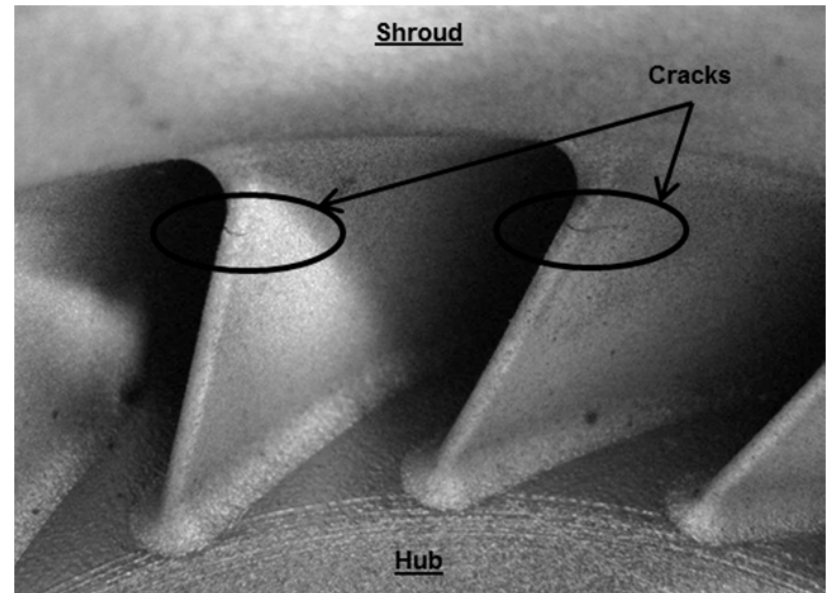
- Jeff Hawk, Albany OR: Material and creep experiments

Industry

- i3D MFG, Bend OR: EOS AM Material

BACKGROUND

Cracks: In conventional and AM parts



[1] 2006 Los Angeles Incident, PROBABLE CAUSE: "The HPT stage 1 disk failed from an intergranular fatigue crack"

<http://aviation-safety.net/database/record.php?id=20060602-0>

[2] Direct Metal Laser Sintering: Karl Wygant et al.; Pump and Turbine 2014

BACKGROUND

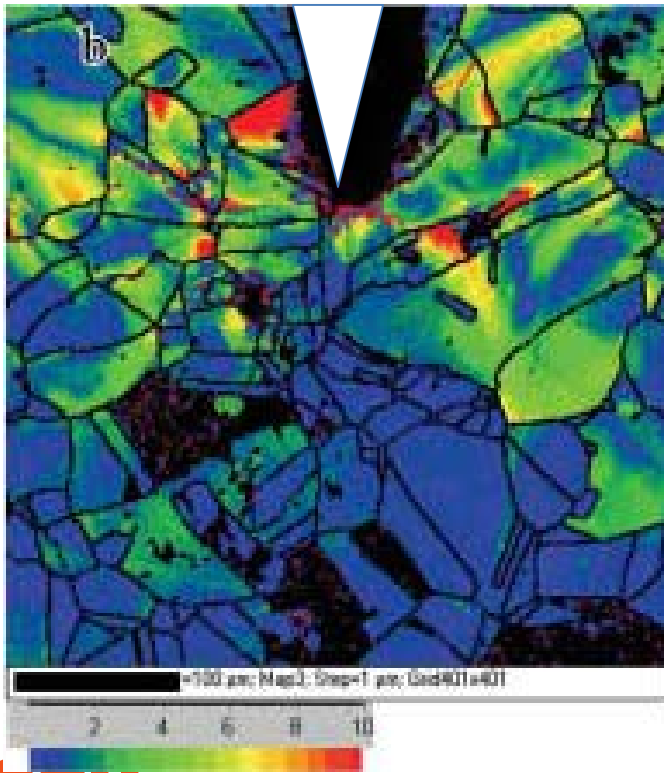
Views on Fatigue Failure

- **S-N:** stress only, no cracks
- **Damage Mechanics**
- **Fracture Mechanics:** cracks, global
Rule based (Paris law and beyond)
- **Micromechanics:** *local description*
Aims to avoid rules and become predictive in complex loading scenarios and with realistic constitutive models

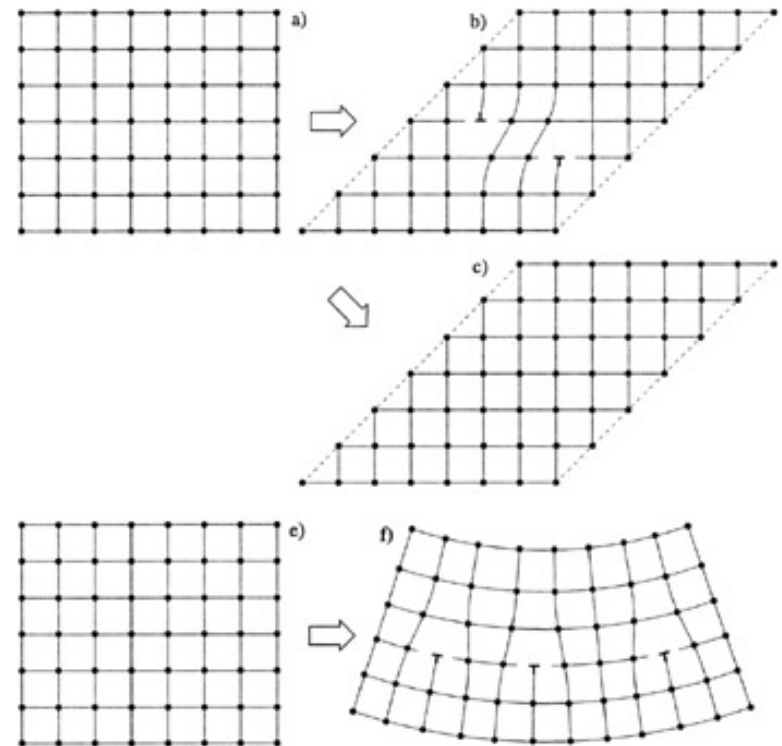
BACKGROUND

Plasticity

EBSD misorientation to reference at crack tip



Misorientation=GND
Strain gradients



BACKGROUND

Crack Tip Plastic Zones

$$r_m = \frac{1}{3\pi} \frac{K}{(\sigma_0)^2} \rightarrow r_c = \frac{1}{3\pi} \frac{K}{(4\sigma_0)^2} \quad \text{.....cyclic plastic zone size}$$

$$\eta = \frac{\Delta \varepsilon_{pl}}{r_c} \quad \text{..... strain gradient, therefore a length } \Lambda [m]$$

$$\varepsilon_{pl}, \eta \rightarrow \sigma_0 = f(\varepsilon_{pl}, \eta, \text{microstr.})$$

$$\Delta a \approx \Delta CMOD = \frac{J}{2\sigma_0} \rightarrow \left(\frac{J}{2\sigma_0} / \Lambda \right) \text{.....non-dim.}$$

BACKGROUND

Hypothesis

Strain Gradient effects of viscoplastic deformation play a relevant role in the failure response of IN718 at 650°C and affect creep-fatigue interaction processes

- Conventional viscoplasticity is incomplete in its description of rate dependent deformation as effects of gradients of strain are ignored.
- Gradient theories predict higher crack tip stresses, and thus stronger activation of stress dependent processes
- Gradient theories alter the tip deformation fields, and thus not only a cyclic plastic zone but also a cyclic gradient zone exist in fatigue

BACKGROUND

Research Questions

- **How do we formulate a constitutive framework that accounts for gradient viscoplasticity and other observed specific features of plasticity in IN718.**
- **What are the experimental methods to determine the lengthscale parameters inherent to a gradient theory through experimentation?**
- **How is a Local-Approach to material failure best be used to predict crack growth in IN718 under creep-fatigue-environmental loading conditions?**
- **How does IN718-CONV differ from IN718-AM?**

OVERVIEW: METHODS

Uniaxial Constitutive Parameters

- Uniaxial tensile tests at various rates and with rate jumps
- Uniaxial creep at various loads and with load jump
- Uniaxial tensile deformation followed by creep

Size Dependent Constitutive Parameters

- High temperature nanoindentation with mN loads
- Hardness and Creep
- Load rate

OVERVIEW: METHODS

Fracture Mechanics

- Fatigue crack growth at 650°C
- Creep crack growth at 650°C
- Creep-Fatigue crack growth at at 650°C
- Fractography

OVERVIEW: METHODS

Computational Mechanics

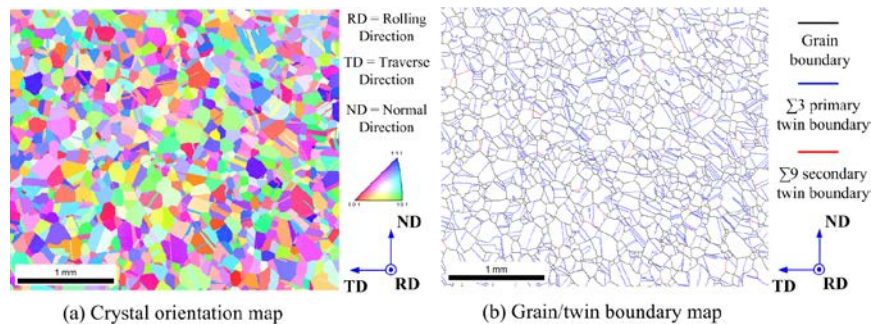
- Constitutive models for viscoplasticity in IN 718
- Norton-law based models
- Dislocation mechanics based models
- Viscoplastic strain gradients
- Structural mechanics
- Crack growth models for fatigue
- Crack growth models for creep
- Crack growth models for creep-fatigue

LEAD KRUZIC

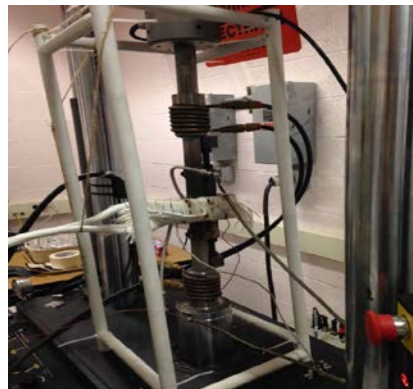
IN 718 Procurement and heat treat

- NETL-Albany provided rolled plate from forged slab
- OSU standard heat treat

IN 718 Microstructure Characterization

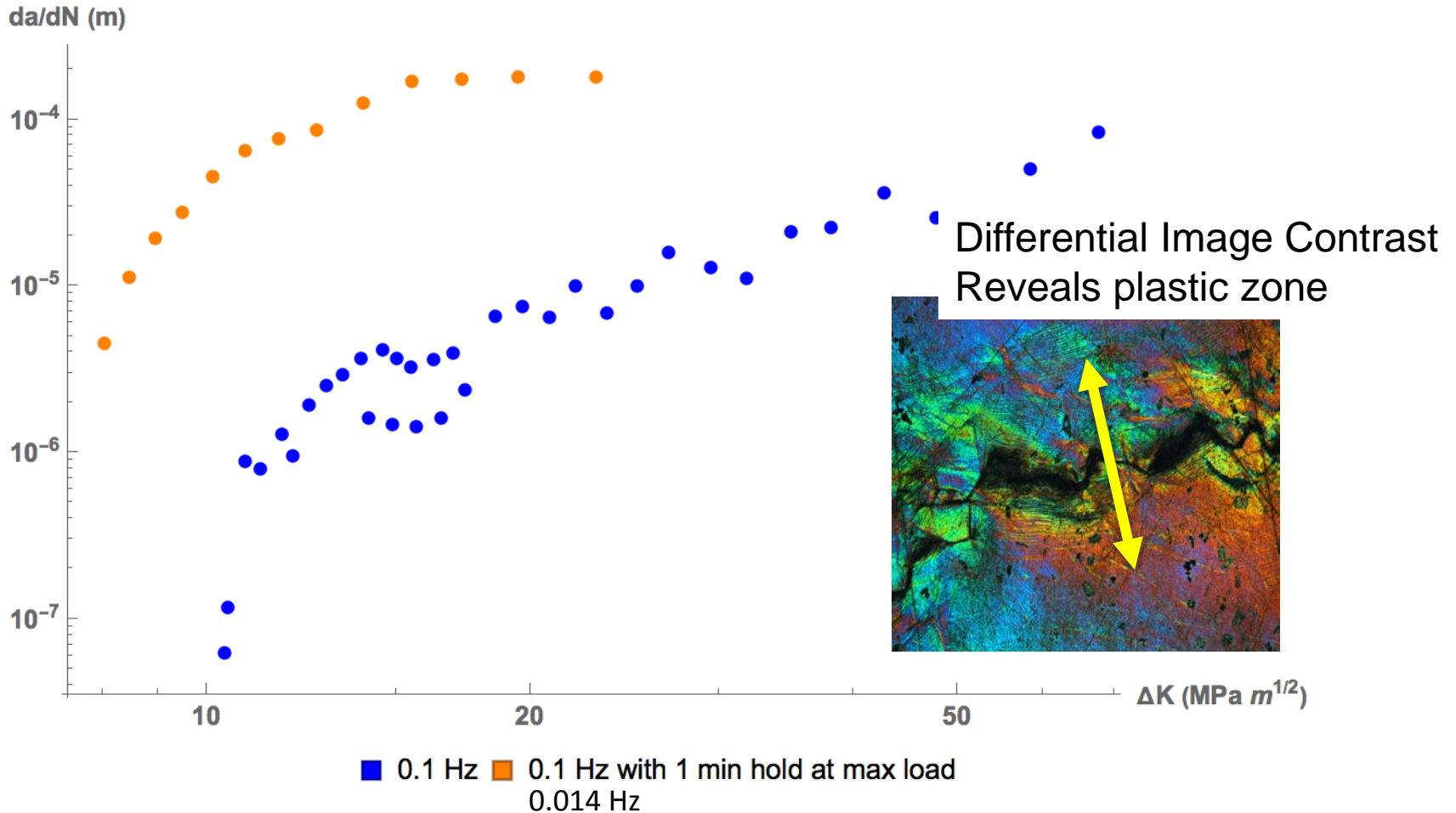


HT Fracture Mechanics Set up



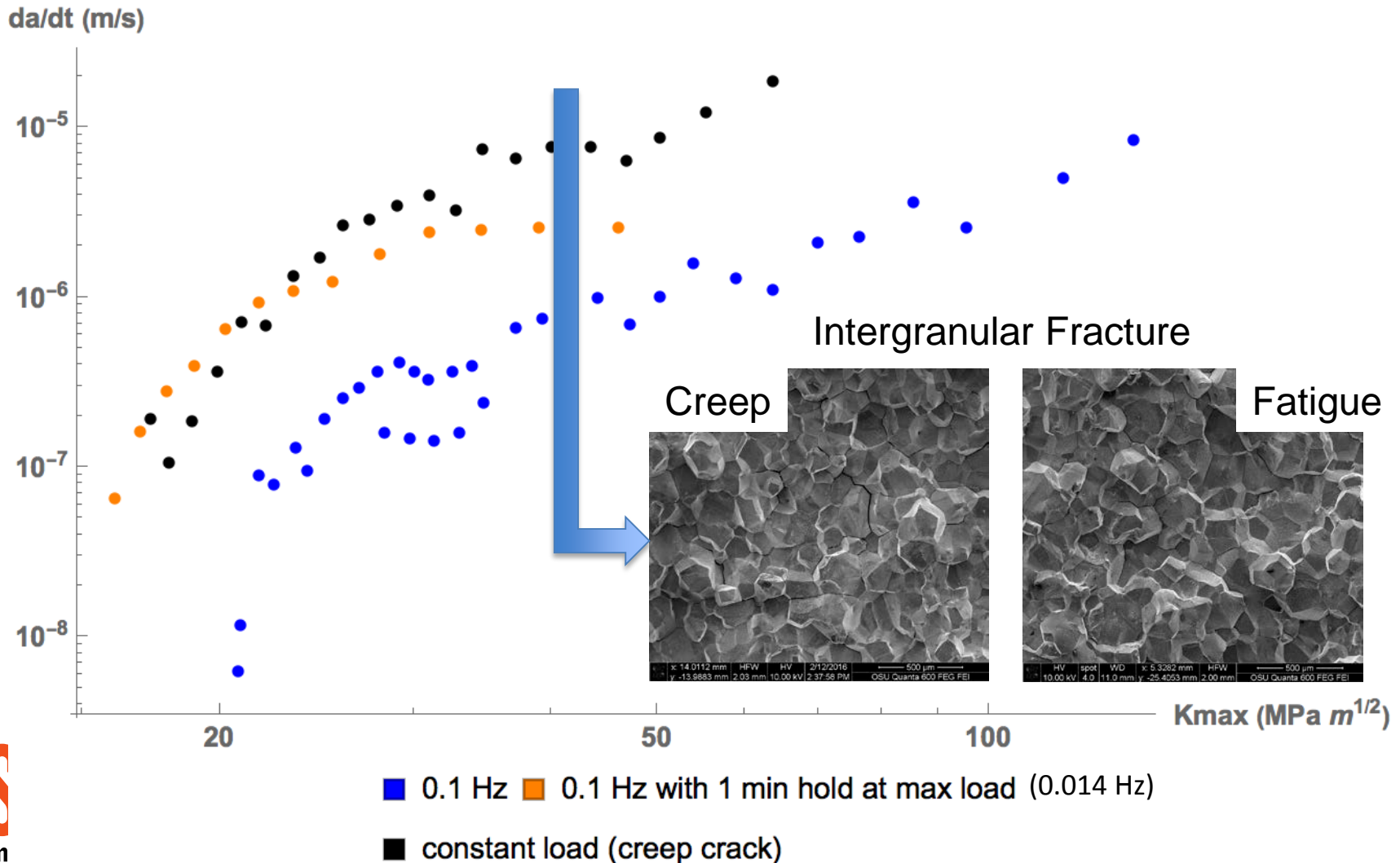
LEAD KRUZIC

Wrought Fatigue Crack Growth Rates
650°C, Air, R = 0.5, Triangle/Trapezoid



LEAD KRUZIC

Wrought Crack Growth Rates as a Function of Time
650°C, Air, Creep or R = 0.5 Triangle

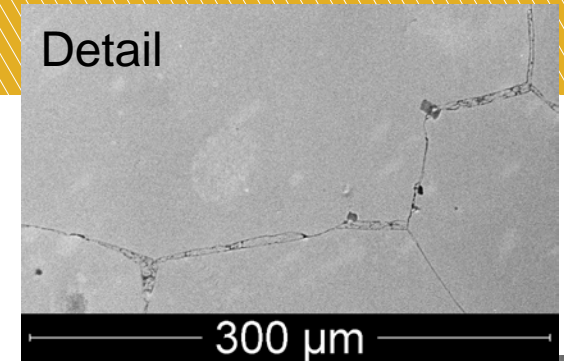


LEAD KRUZIC

Crack growth mechanism

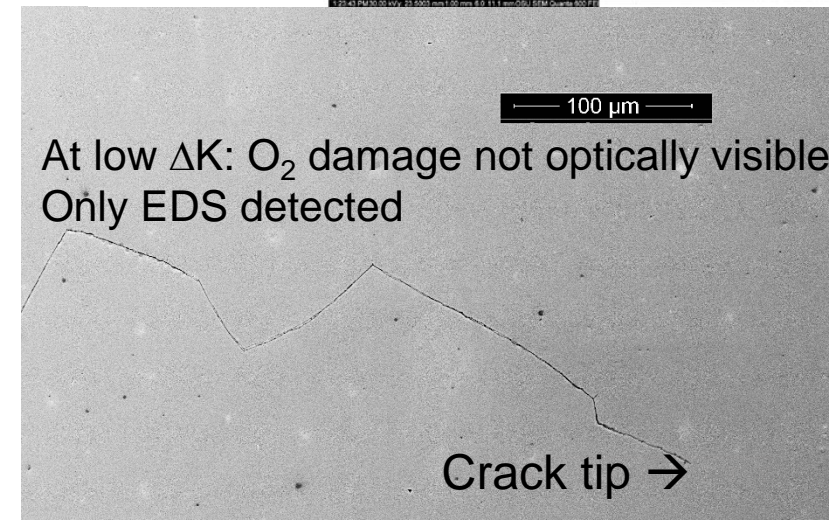
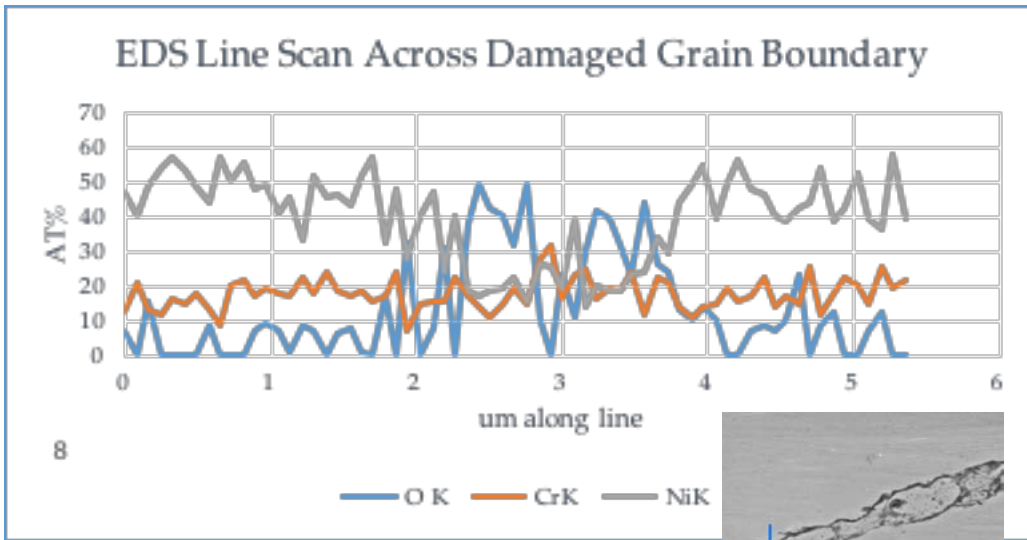
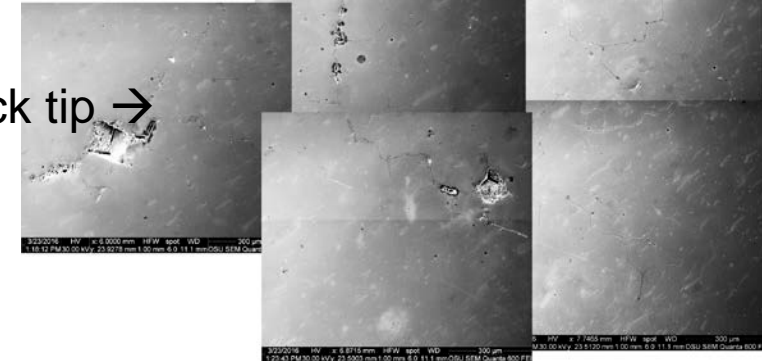
(for CREEP AND LOW FREQ.)

- stress assisted grain boundary oxidation (SAGBO)
- Coupled with plastic deformation

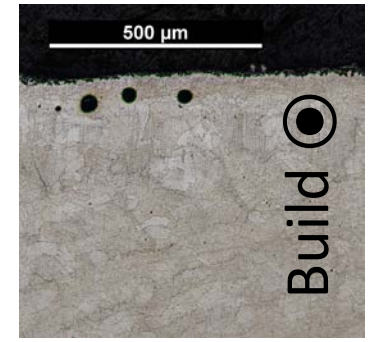
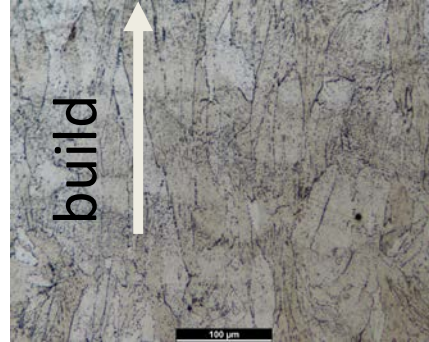
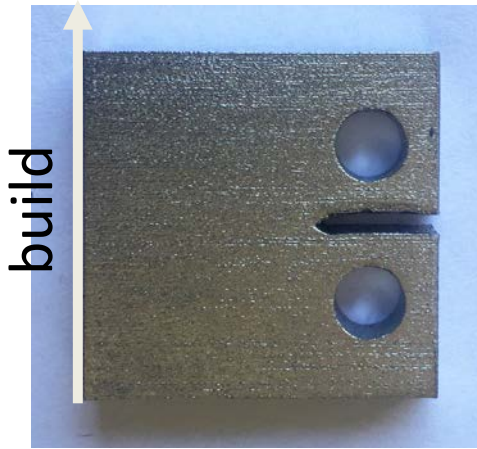


At high ΔK : O₂ damage optically visible

Crack tip →



LEAD KRUZIC



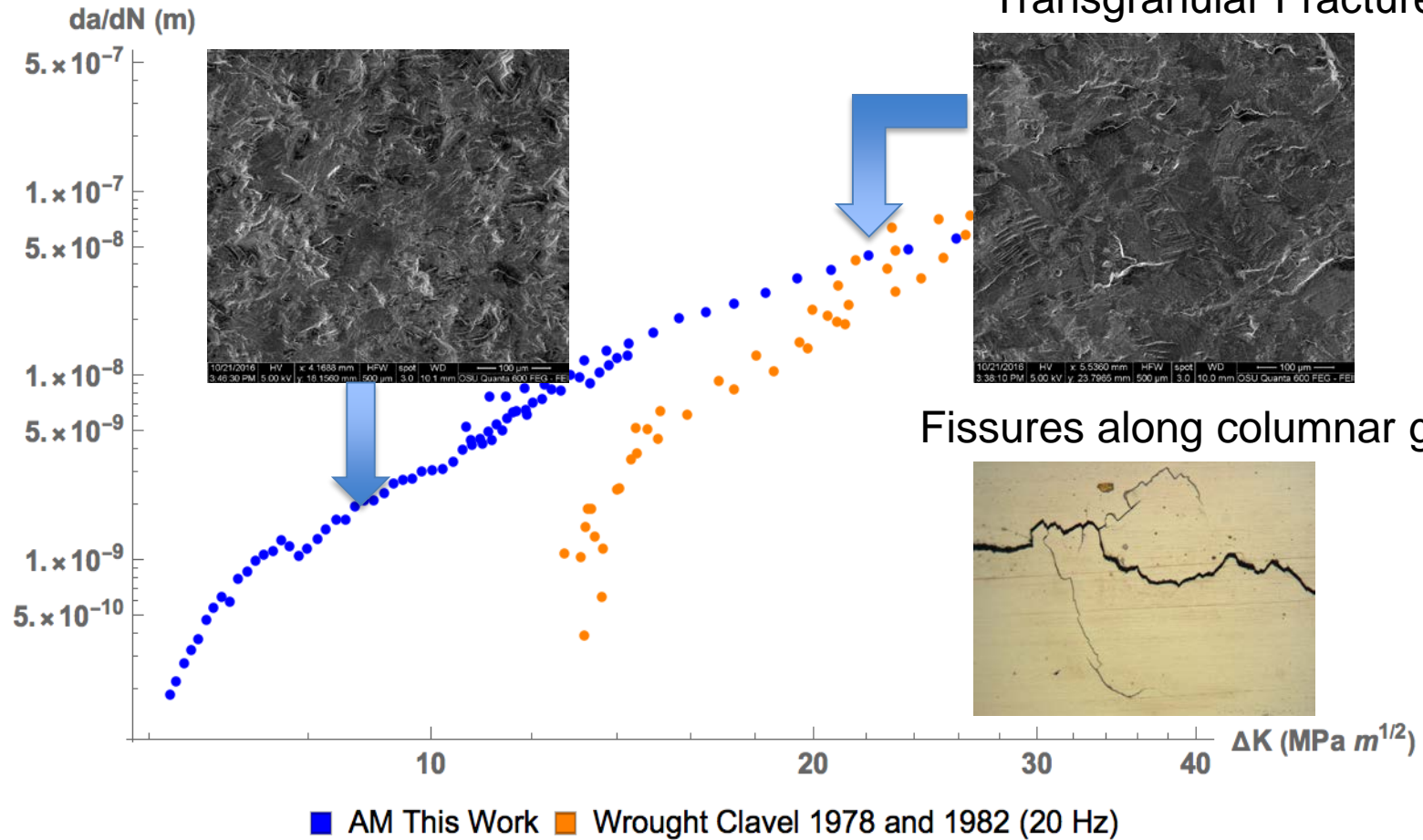
Direct metal laser sintered (DMLS) alloy 718 samples:

- EOS M290 printer
- Pre-alloyed 718 powder supplied by EOS
- Argon build environment
- 40 μm layer height
- EOS proprietary scan pattern (63° rotation between layers)
- For this work: heat treatment steps identical to wrought material tested here (AMS 5662)
- We believe this is representative of commercially available high quality prints



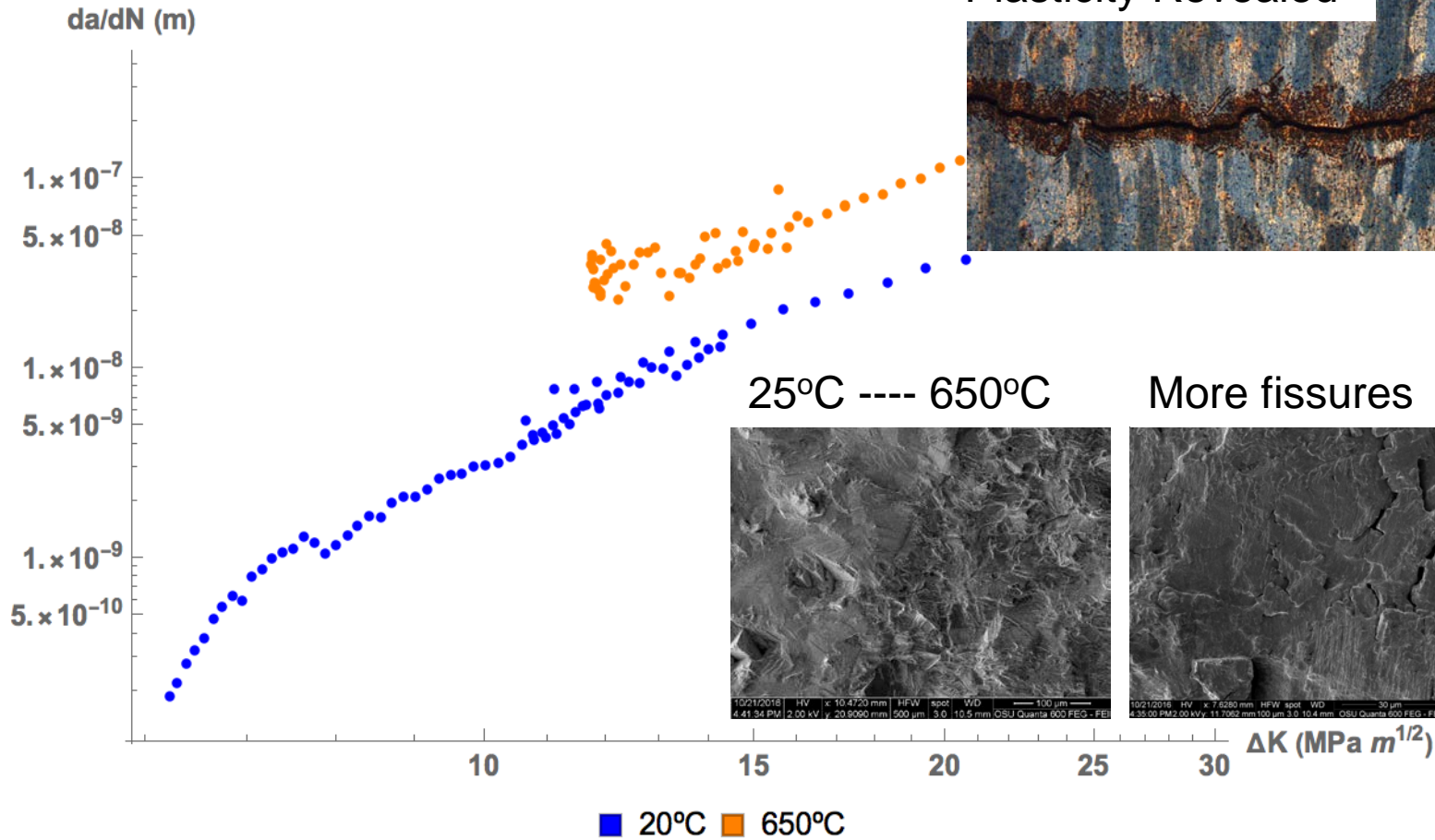
LEAD KRUZIC

AM Fatigue Crack Growth Rates at 20°C
30 Hz, R = 0.1, Sine



LEAD KRUZIC

AM Fatigue Crack Growth Rates
30 Hz, R = 0.1, Sine



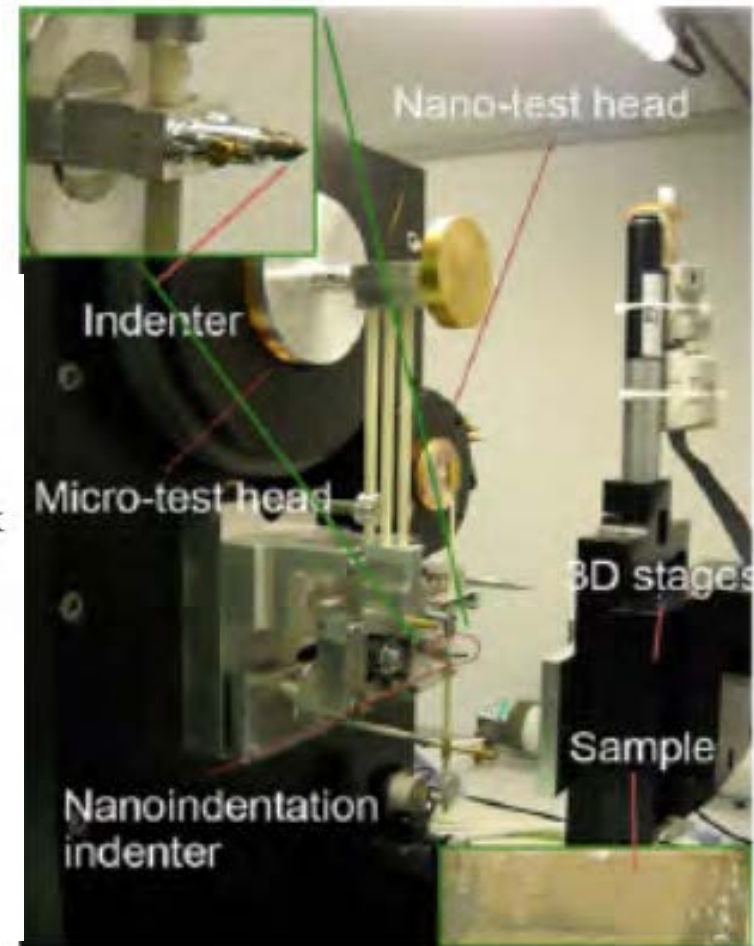
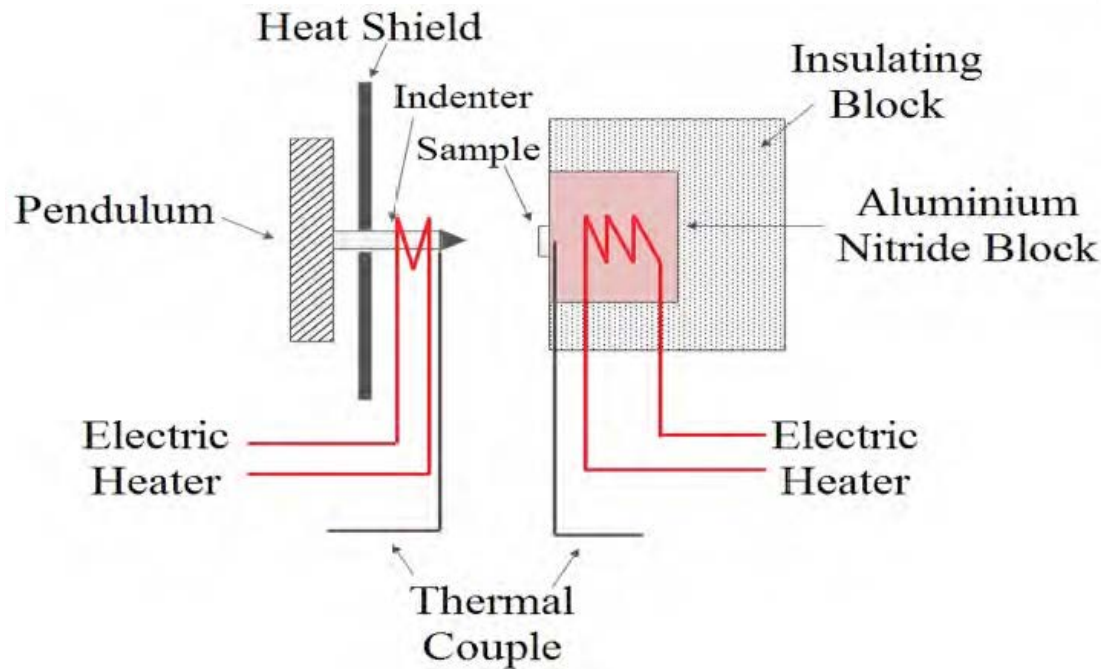
LEAD KRUZIC

Crack Growth Experiments

- At low frequency (for IN718CONV):
 - Intergranular fracture together with plasticity
 - Time dominates
- At high frequency (for IN718AM):
 - Transgranular fracture together with plasticity
 - Cycling dominates
- CONV vs. AM:
 - Equiaxed grains vs. columnar grains
 - ΔK_{th} is much reduced in AM & $\Delta a/\Delta N$ elevated in AM even if tensile properties are good

LEAD TOMAR

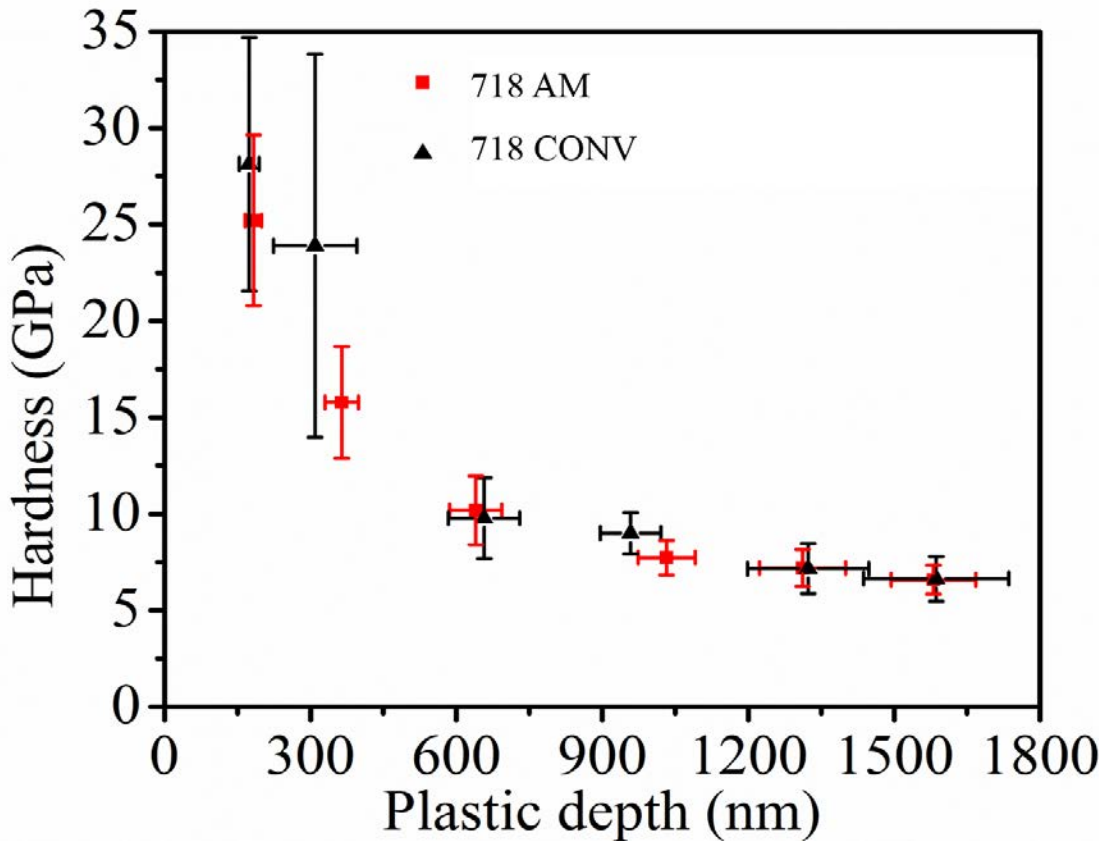
High Temperature Nanoindentation Probe viscoplasticity at small length scales



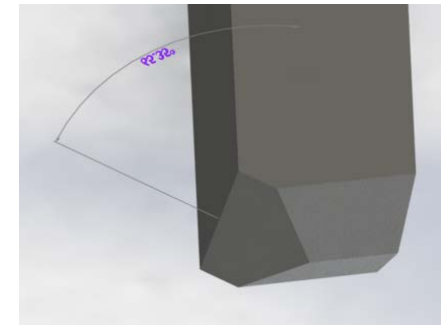
LEAD TOMAR

Hardness is Load Dependent

This is a key finding which confirms a key hypothesis:
Plastic deformation at high temperatures is size dependent



Smaller

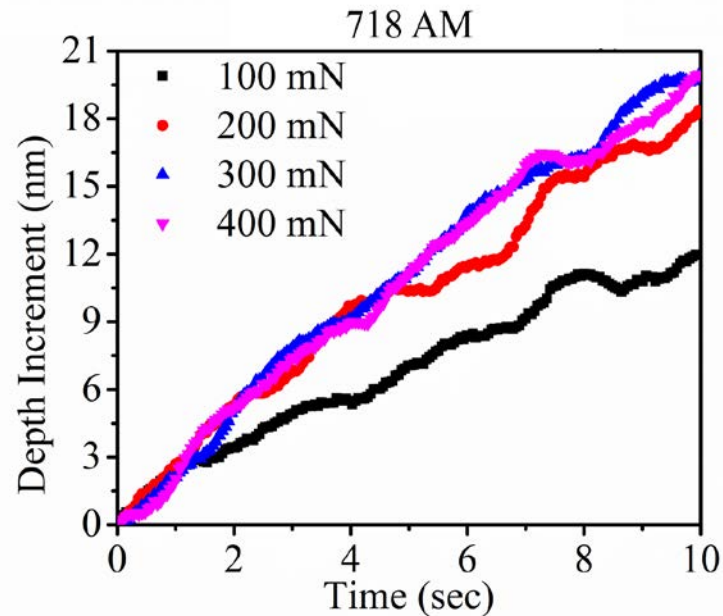
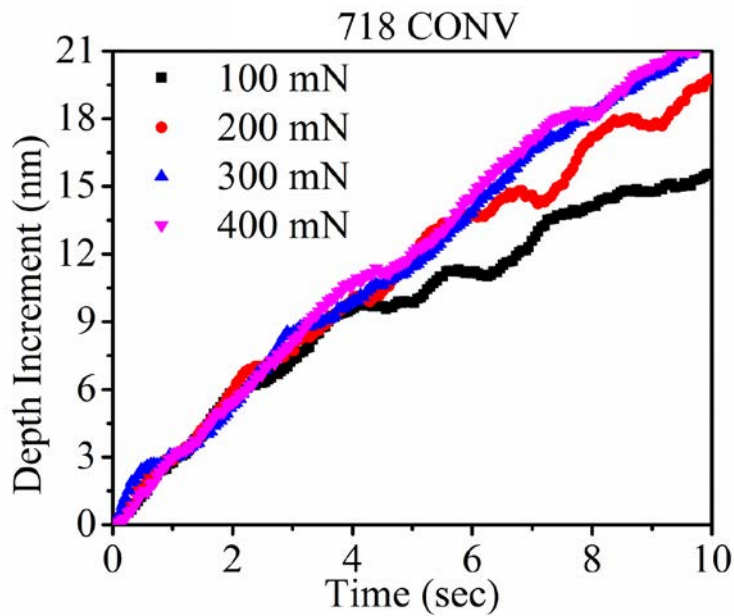


Berkovich Indenter
C-BN

LEAD TOMAR

Creep (short term) is Load Dependent

This is a key finding which confirms a key hypothesis:
Creep deformation at high temperatures is size dependent



Smaller

LEAD TOMAR

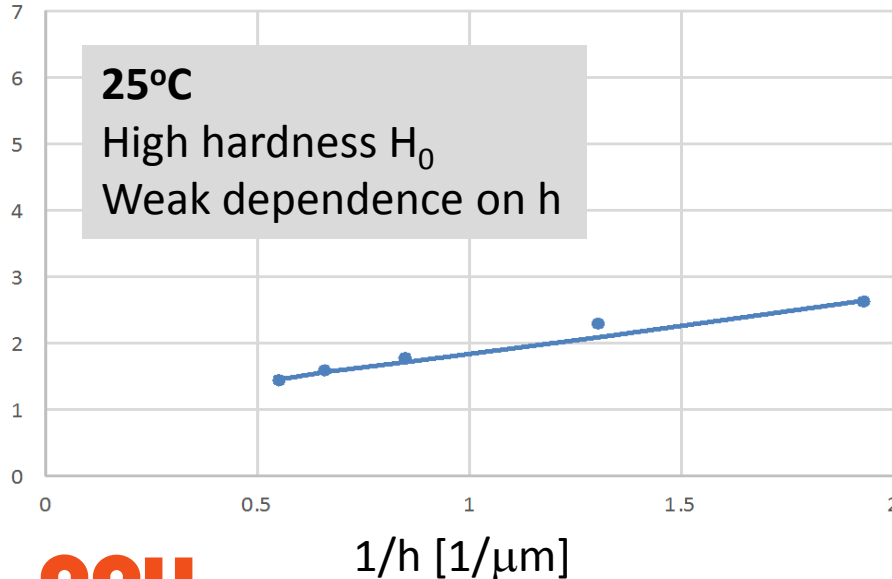
Strain Gradient Plasticity Theory:

Hardness (H) is indentation depth (h) dependent:

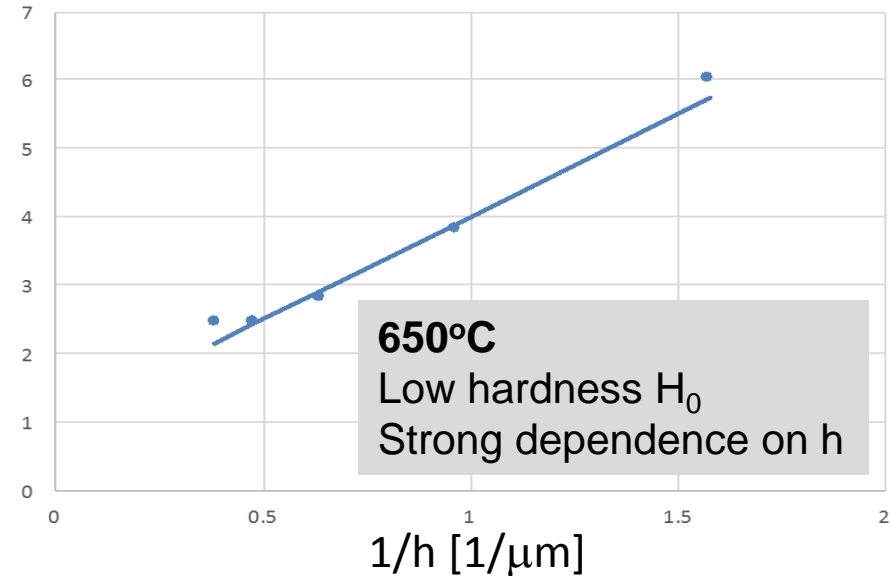
$$\left(\frac{H}{H_0}\right) = 1 + \frac{h^*}{h}$$

	H_0	h^*
25°C	6 GPa	0.8 μm
650°C	3 GPa	3.0 μm

$(H/H_0)^2$ 25C: $H_0=6$ GPa, $h^*=0.8$ μm



$(H/H_0)^2$ 650C: $H_0=3$ GPa, $h^*=3$ μm



LEAD TOMAR

Plasticity at Small Scales

- IN718 exhibits a dependence of hardness of indentation depth at 650°C confirming a key hypothesis
- IN718 exhibits a dependence of creep on indentation load at 650°C confirming a key hypothesis
- Hardness and its size dependence was similar for the CONV and AM version of IN718
- Hardness follows a model strain gradient plasticity
- While hardness is lower at 650°C than at 25°C, the dependence of hardness of indentation depth is stronger at 650°C

Computational Mechanics

Constitutive Models:

- **Strain Gradient Viscoplastic Theory as justified by indentation experiments**
- **Tension-compression asymmetric yield theory**

Crack Growth Models:

- **Micromechanical models combining material separation and plastic deformation as justified by crack growth experiments**
- **Cohesive Zone Model**

LEAD SIEGMUND

Unified Viscoplastic Constitutive Models With Strain Gradients

Flow stress

$$\sigma_{\text{flow}} = \sigma_0 + M\alpha\mu b\sqrt{\rho}$$

σ_0 : stress related to lattice friction and solute contents

M : average Taylor factor ($M \approx 3$)

α : weighting factor of dislocation interactions ($\alpha \approx 1/3$)

μ : shear modulus

b : Burgers vector

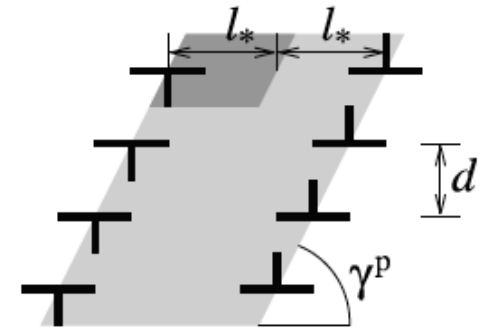
LEAD SIEGMUND

Dislocations: Carriers of Plastic Deformation

Dislocation density: $\rho = \rho_S + \rho_G$

- Statistically stored dislocation:

$$\rho_S = \frac{\sqrt{3}\bar{\epsilon}^{vp}}{b\Lambda}$$

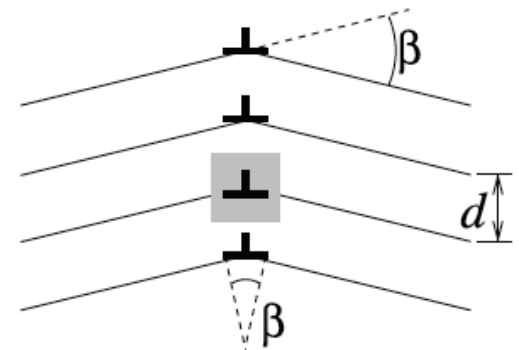


- Geometrically necessary dislocation:

$$\rho_G = \bar{r} \frac{\bar{\eta}}{b}$$

$\bar{\eta}$: effective plastic strain gradient

\bar{r} : Nye-factor ($\bar{r} = 1.90$)



LEAD SIEGMUND

Dislocation Density based Constitutive Model

Total strain rate $\dot{\boldsymbol{\varepsilon}} = \dot{\boldsymbol{\varepsilon}}^e + \dot{\boldsymbol{\varepsilon}}^{vp}$	
Elastic strain rate: $\dot{\boldsymbol{\sigma}} = \mathbf{D}\dot{\boldsymbol{\varepsilon}}^e$ Elasticity tensor $D_{ijkl} = \mu(\delta_{ik}\delta_{jl} + \delta_{il}\delta_{jk}) + \lambda\delta_{ij}\delta_{kl}$ Lamé's coefficients: λ, μ	Viscoplastic strain rate: $\dot{\boldsymbol{\varepsilon}}^{vp} = \frac{\partial \phi}{\partial \boldsymbol{\sigma}}$ Isotropic material $\bar{\sigma} = f(\boldsymbol{\sigma}) = \sqrt{\frac{3}{2}} \mathbf{s} : \mathbf{s}$ $\dot{W}^{vp} = \bar{\sigma} \dot{\bar{\varepsilon}}^{vp} = \boldsymbol{\sigma} : \dot{\boldsymbol{\varepsilon}}^{vp}$

Kinetic equation $\frac{\bar{\sigma}}{\sigma_{ref}} = \left(\frac{\dot{\bar{\varepsilon}}^{vp}}{\dot{\varepsilon}_0} \right)^{1/m}$	
Taylor equation $\sigma_{ref} = \sigma_0 + M\alpha\mu b\sqrt{\rho}$	
Dislocation density: $\rho = \rho_s + \rho_G$	
Statistically stored dislocation $\rho_s = \rho_s^+ + \rho_s^-$ <ul style="list-style-type: none"> - Accumulation: $\frac{d\rho_s^+}{d\bar{\varepsilon}^{vp}} = Mk_1\sqrt{\rho_s + \rho_G}$ - Dynamic recovery: $\frac{d\rho_s^-}{d\bar{\varepsilon}^{vp}} = Mk_2\rho_s$ Strain rate sensitivity $k_2 = k_{20} \left(\frac{\dot{\bar{\varepsilon}}^{vp}}{\dot{\varepsilon}_0} \right)^{-1/n}$	Geometrically necessary dislocation $\rho_G = \bar{r} \frac{\bar{\eta}^{vp}}{b}$ Effective strain gradient $\bar{\eta}^{vp} = \sqrt{\frac{1}{4} \eta_{ijk}^{vp} \eta_{ijk}^{vp}}$ $\eta_{ijk}^{vp} = \varepsilon_{ik,j}^{vp} + \varepsilon_{jk,i}^{vp} - \varepsilon_{ij,k}^{vp}$

LEAD SIEGMUND

FE Implementation (UMAT for ABAQUS)

At the time step $[t_n, t_{n+1}]$, quantities $(\sigma, \varepsilon, \bar{\varepsilon}^{vp}, \rho_s, \rho_G, \sigma_{ref}, \Delta t)_n$ are given.

Step 1. Loop

1.1 Calculate viscoplastic strain increment (explicit Euler method): $\Delta \bar{\varepsilon}^{vp} = \dot{\bar{\varepsilon}}_n^{vp} \Delta t$

1.2 Update state variables

SSD density:

$$\begin{aligned} (\rho_s)_{n+1} &= (\rho_s^+)_{n+1} + (\rho_s^-)_{n+1} & (\rho_s^+)_{n+1} &= (\rho_s^+)_{n+1} + \Delta \rho_s^+ & \Delta \rho_s^+ &= \Delta \bar{\varepsilon}^{vp} M k_1 \sqrt{(\rho_s)_n + (\rho_G)_n} \\ & & (\rho_s^-)_{n+1} &= (\rho_s^-)_{n+1} + \Delta \rho_s^- & \Delta \rho_s^- &= \Delta \bar{\varepsilon}^{vp} M k_2 (\rho_s)_n \end{aligned}$$

GND density:

$$\begin{aligned} (\rho_s)_{n+1} &= \bar{r} \frac{(\bar{\eta}^{vp})_n}{b} & (\bar{\eta}^{vp})_{n+1} &= (\bar{\eta}^{vp})_n + \Delta \bar{\eta}^{vp} & \Delta \bar{\eta}^{vp} &= \sqrt{\frac{1}{4} (\Delta \eta_{ijk}^{vp})_n (\Delta \eta_{ijk}^{vp})_n} \\ & & (\Delta \eta_{ijk}^{vp})_n &= \left(\frac{\partial N_I}{\partial X_j} (\Delta \varepsilon_{ik}^{vp})_I + \frac{\partial N_I}{\partial X_i} (\Delta \varepsilon_{jk}^{vp})_I - \frac{\partial N_I}{\partial X_k} (\Delta \varepsilon_{ij}^{vp})_I \right)_n \end{aligned}$$

Reference stress:

$$(\sigma_{ref})_{n+1} = \sigma_0 + M \alpha \mu b \sqrt{(\rho_s)_{n+1} + (\rho_G)_{n+1}}$$

1.3 Solve a nonlinear equation for stress using a Newton-Raphson scheme

$$f(\Delta \bar{\sigma}) = 3\mu(\bar{\varepsilon} - \Delta \bar{\varepsilon}^{vp}) - (\bar{\sigma}_n + \Delta \bar{\sigma}) = 0$$

1.4 Check convergence criterion for the k -th iteration: $\left| \frac{\Delta \bar{\sigma}_{(k+1)} - \Delta \bar{\sigma}_{(k)}}{\Delta \bar{\sigma}_{(k+1)}} \right| \leq \text{TOL}$

if satisfied go to Step 2 otherwise go to 1.1.

Step 2. Update stress tensor and viscoplastic strain

$$\text{Stress tensor } s_{ij} = \frac{2\mu}{1 + \frac{3\mu}{(\bar{\sigma}_n + \Delta \bar{\sigma})} \Delta \bar{\varepsilon}^{vp}} \hat{e}_{ij} \quad \text{Viscoplastic strain } \bar{\varepsilon}_{n+1}^{vp} = \bar{\varepsilon}_n^{vp} + \Delta \bar{\varepsilon}^{vp}$$

Step 3. Compute the material Jacobian $C = \partial \Delta \sigma / \partial \Delta \varepsilon$

NUMERICAL EXAMPLES

Annular non-uniform thickness rotating disc

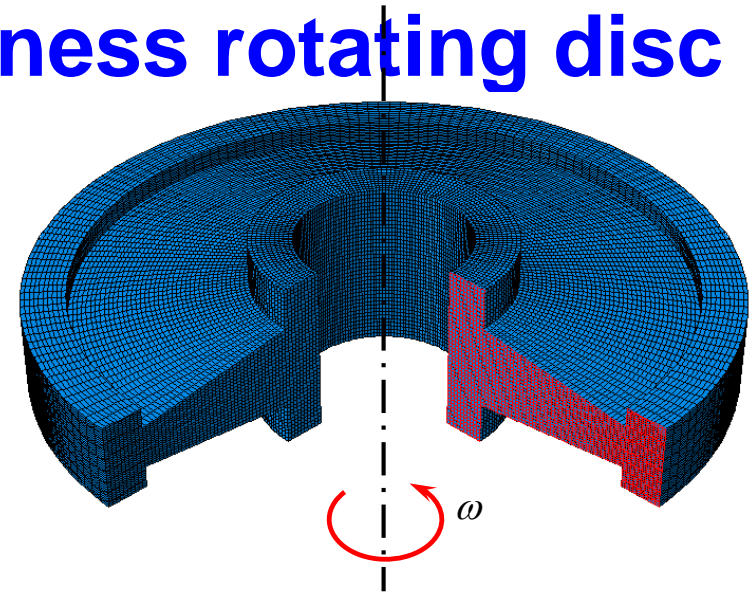
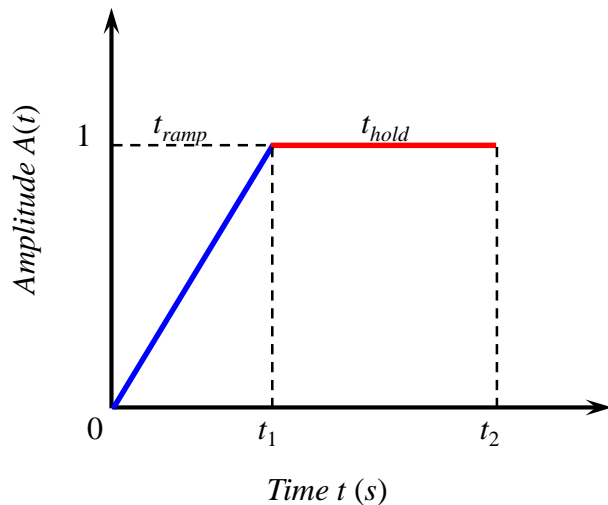
- FE model

- Axisymmetric conditions
- Mass density $\delta = 8.220 \cdot 10^{-3} \text{ g/mm}^3$
- Loading: centrifugal loading (body force)

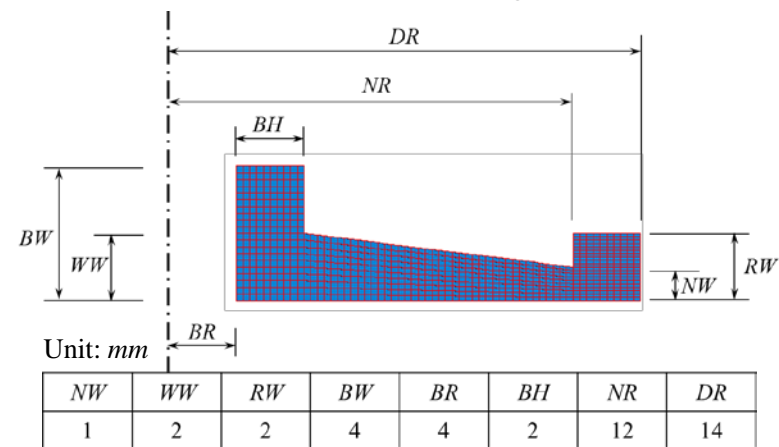
Angular velocity: $\omega(t) = A(t)\omega_0$

with $\omega_0 = 26179.9 \text{ rad/s}$ (250,000 RPM)

$t_{\text{ramp}} = 600 \text{ s}$, $t_{\text{hold}} = 10^5 \text{ s}$



Non-uniform annular rotating disc



- Generic material data for SG-KM model

E (GPa)	ν	σ_0 (MPa)	m	n	k_1 (mm^{-1})	k_{20}	M	α	b (nm)	$\frac{\sigma}{E}$ (s^{-1})
77.9	0.3	779	25	5	8e5	28.29	1.73	0.3	0.25	1e-3

2D axisymmetric model

NUMERICAL EXAMPLES

Annular uniform thickness rotating disc

- Elastic solution

- Radial stress as a function of distance r from the central axis:

$$\sigma_r(r) = \frac{3+\nu}{8} \delta \omega^2 \left(R^2 + R_0^2 - \frac{R^2 R_0^2}{r^2} - r^2 \right)$$

- Hoop stress as a function of distance r from the central axis:

$$\sigma_t(r) = \frac{1}{8} \delta \omega^2 \left[(3+\nu) \left(R^2 + R_0^2 - \frac{R^2 R_0^2}{r^2} \right) - (1+3\nu) r^2 \right]$$

- Maximum radial stress occurs at $r = \sqrt{RR_0}$

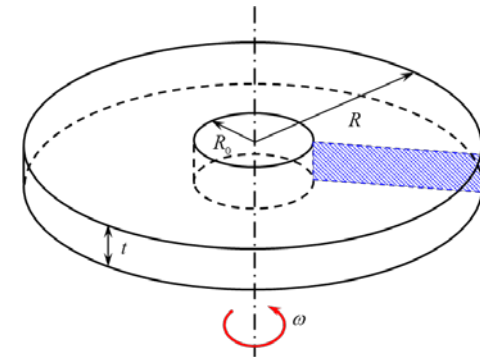
$$\sigma_{r,\max} = \frac{3+\nu}{8} \delta \omega^2 (R - R_0)^2$$

- Maximum radial stress occurs at the perimeter of the hole

$$\sigma_{t,\max} = \frac{1}{4} \delta \omega^2 \left[(3+\nu) R^2 + (1-\nu) R_0^2 \right]$$

- Radial displacement

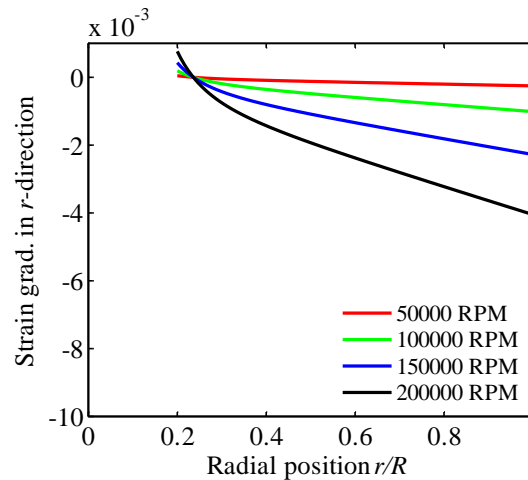
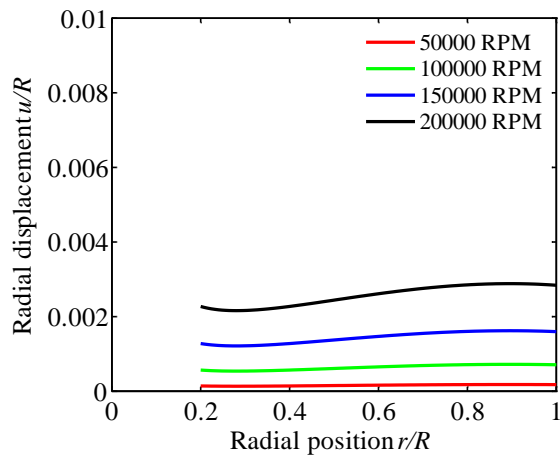
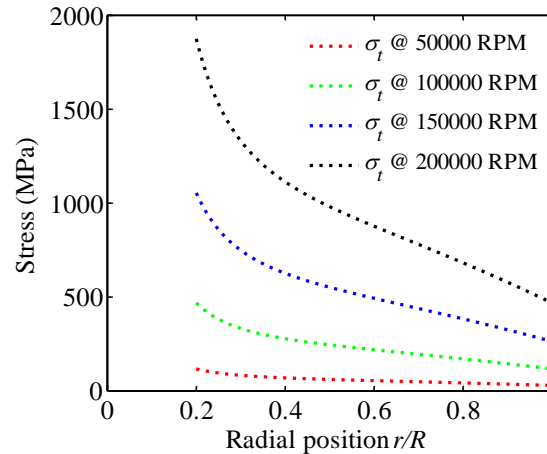
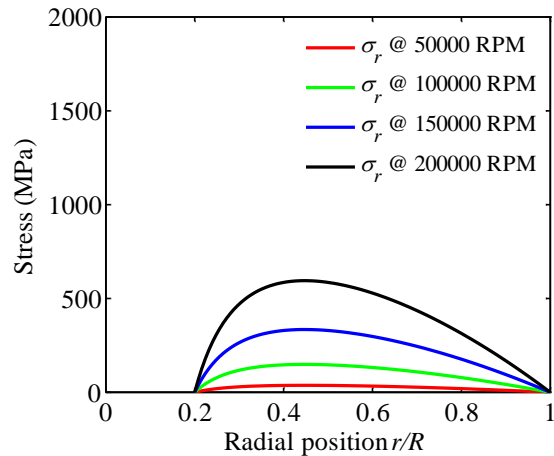
$$u_r = \frac{1}{8} r \delta \omega^2 \frac{(3+\nu)(1-\nu)}{E} \left[R^2 + R_0^2 + \frac{1+\nu}{1-\nu} \frac{R^2 R_0^2}{r^2} - \frac{1+\nu}{3+\nu} r^2 \right]$$



δ density
 E Young's modulus
 ν Poisson's ratio

NUMERICAL EXAMPLES

Annular uniform thickness rotating disc



**Strain Gradients
from centrifugal
forces:
Does this matter?**

LEAD SIEGMUND

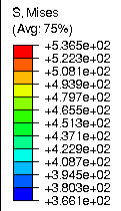
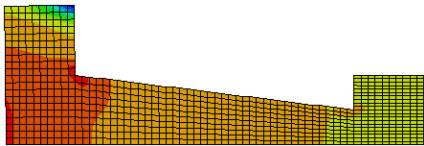
After a hold time of $t_{\text{hold}} = 10^5$ s

Norton

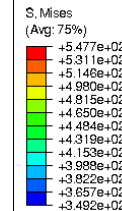
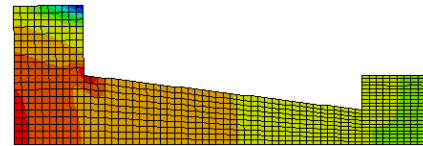
Kocks-Mecking (KM)

SG-KM

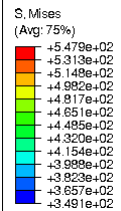
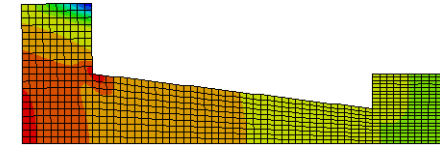
Von Mises stress



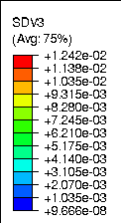
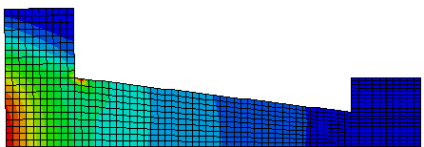
Von Mises stress



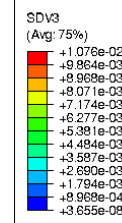
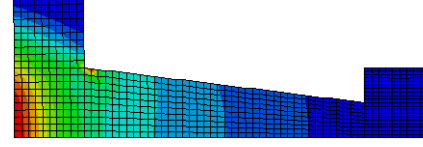
Von Mises stress



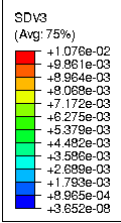
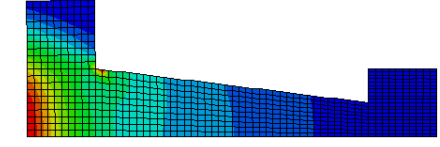
Creep strain



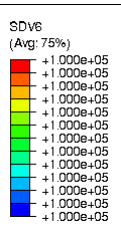
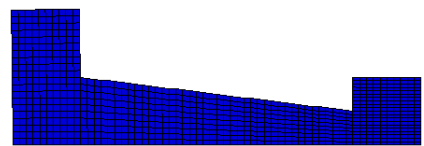
Creep strain



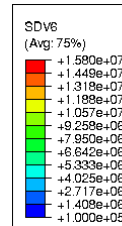
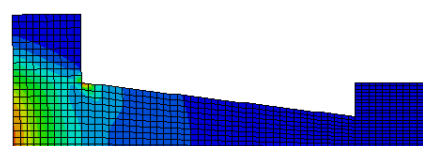
Creep strain



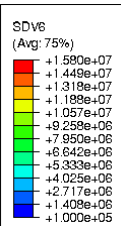
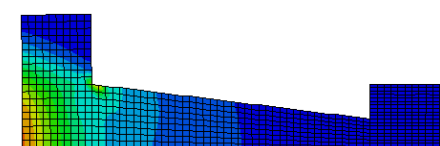
SSD



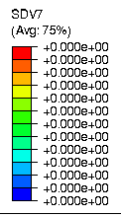
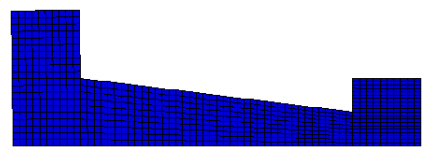
SSD



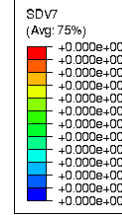
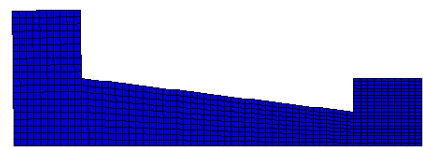
SSD



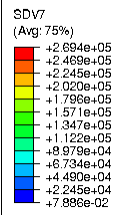
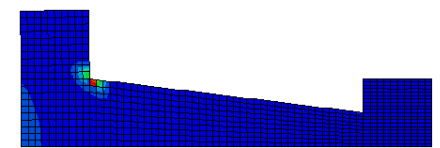
GND



GND

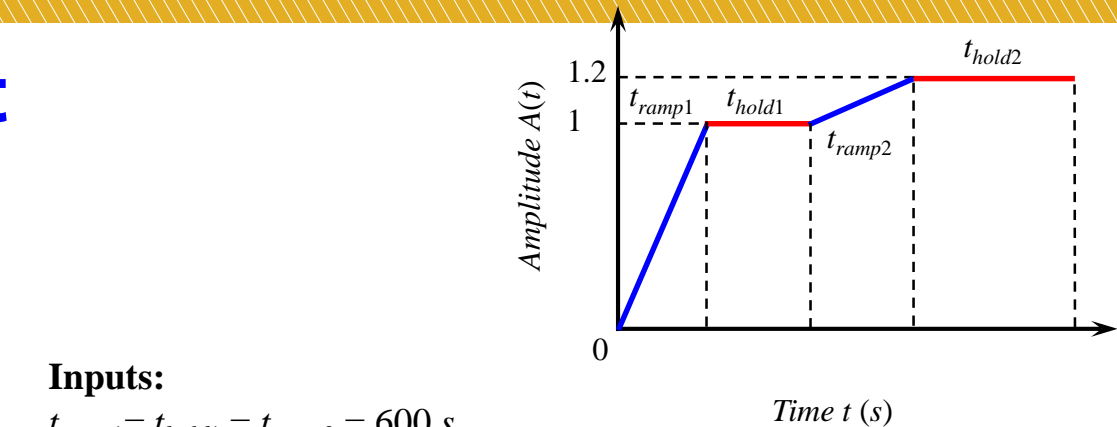
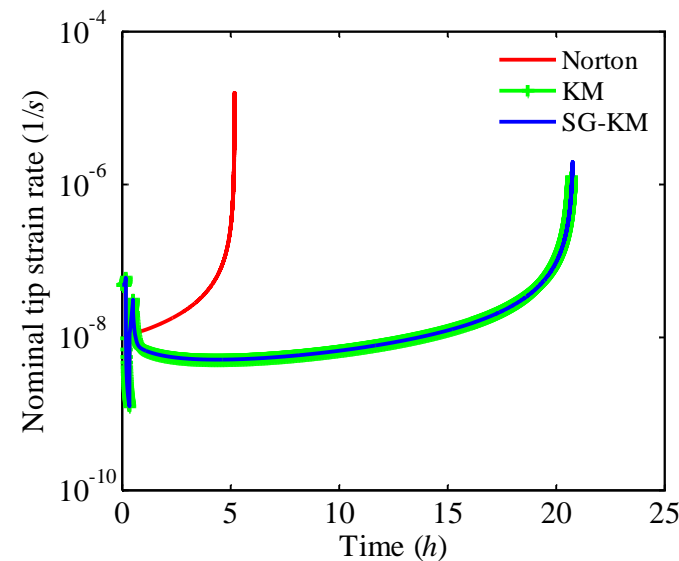
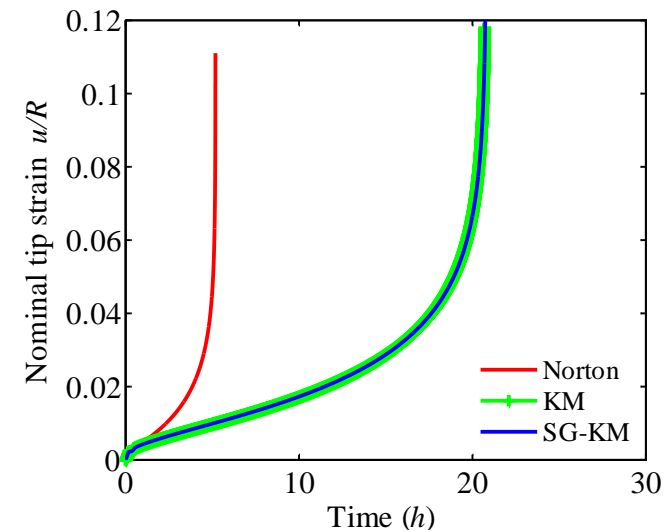


GND



CONSTITUTIVE MODELING

Tip displacement



Inputs:

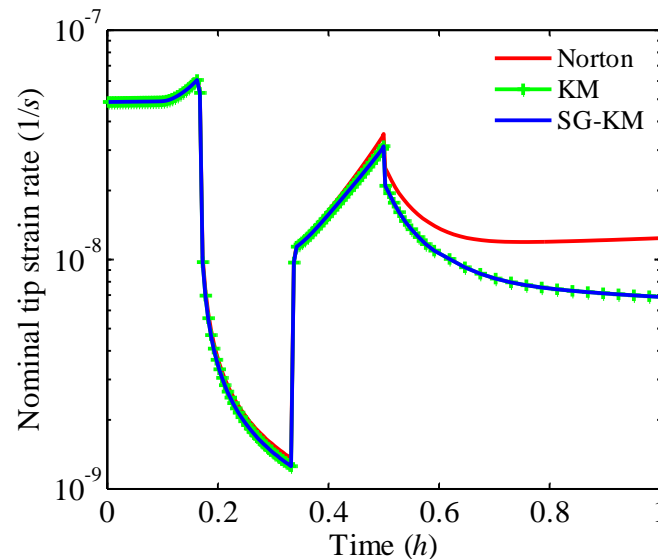
$$t_{ramp1} = t_{hold1} = t_{ramp2} = 600 \text{ s}$$

Ramp 1: from 0 to 250,000 RPM in 600 s

Hold 1: 600 s

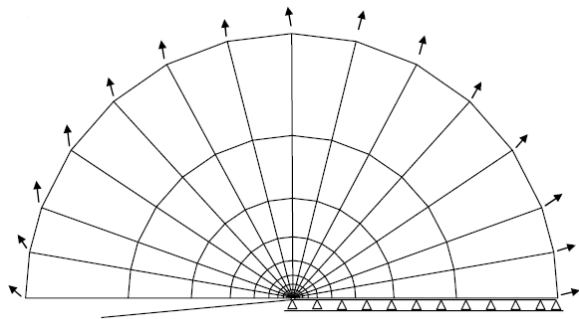
Ramp 2: from 250,000 RPM to 300,000 RPM in 600 s

Hold 2: until failure



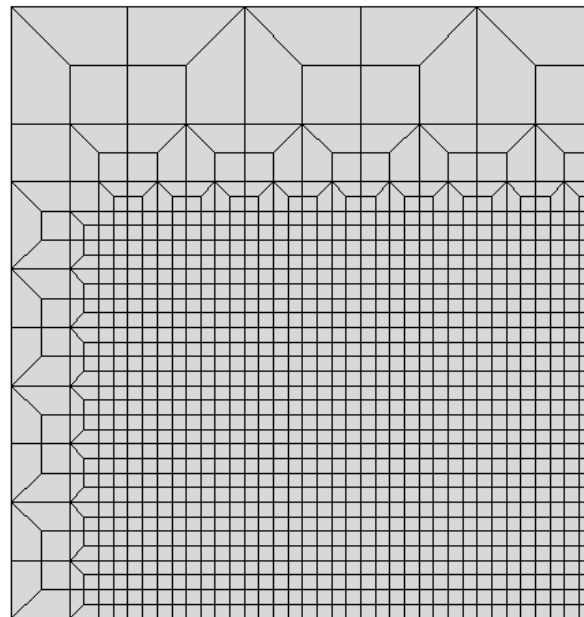
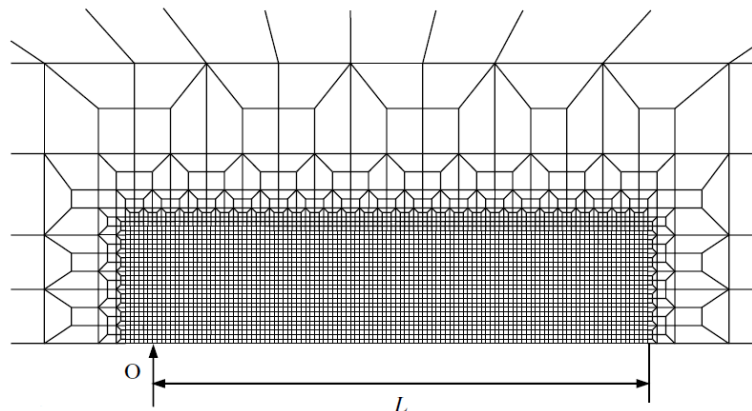
NUMERICAL EXAMPLES

Crack tip fields under creep condition



$$u_x(t) = K_I(t) \sqrt{\frac{r}{2\pi}} \frac{1+\nu}{E} (3-4\nu - \cos\theta) \cos\frac{\theta}{2}$$

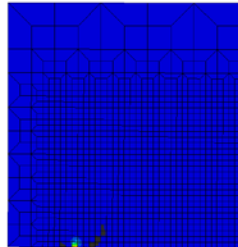
$$u_y(t) = K_I(t) \sqrt{\frac{r}{2\pi}} \frac{1+\nu}{E} (3-4\nu - \cos\theta) \sin\frac{\theta}{2}$$



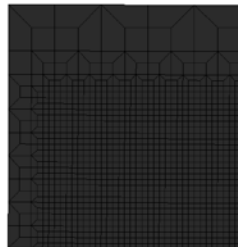
NUMERICAL EXAMPLES

At a ramp time ($t_{\text{ramp}} = 1 \text{ s}$)

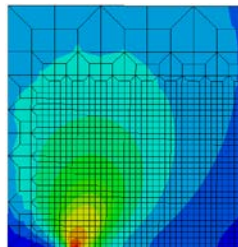
Kocks-Mecking



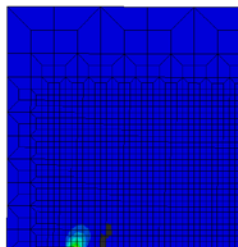
SSD



GND

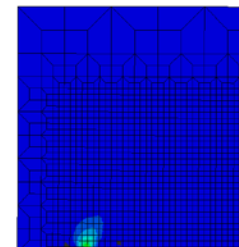
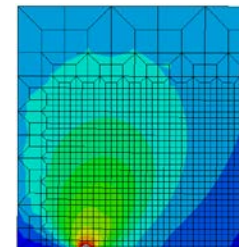
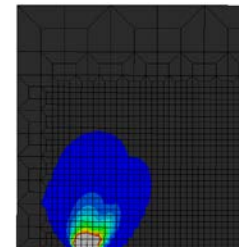
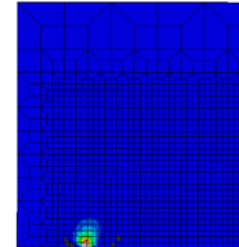


Von Mises stress



Plastic strain

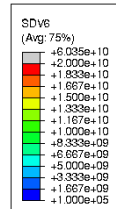
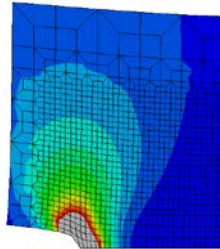
SG-KM



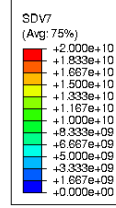
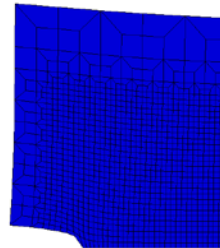
NUMERICAL EXAMPLES

After a hold time of $t_{\text{hold}} = 40 \text{ s}$

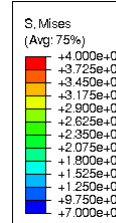
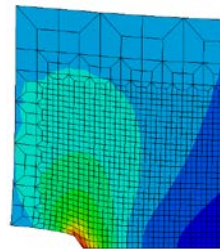
Kocks-Mecking



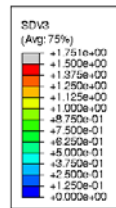
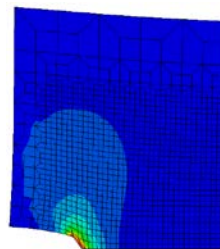
SSD



GND

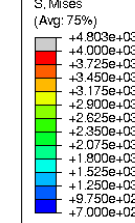
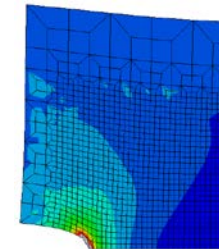
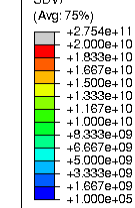
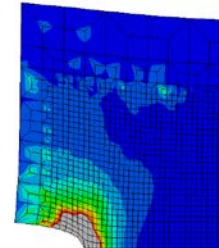
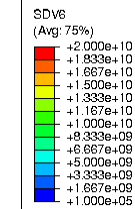
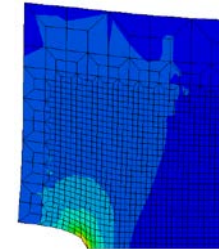


Von Mises stress



Plastic strain

SG-KM



LEAD SIEGMUND

Creep-Fatigue Crack Growth

- **Fatigue damage and creep damage evolve independently and act additively**
- **Embedded in FEM as a Cohesive Zone Model**
 - **Cyclic damage law (Roe-Siegmund)**
 - **Time damage law (Kachanov-Robotnov)**

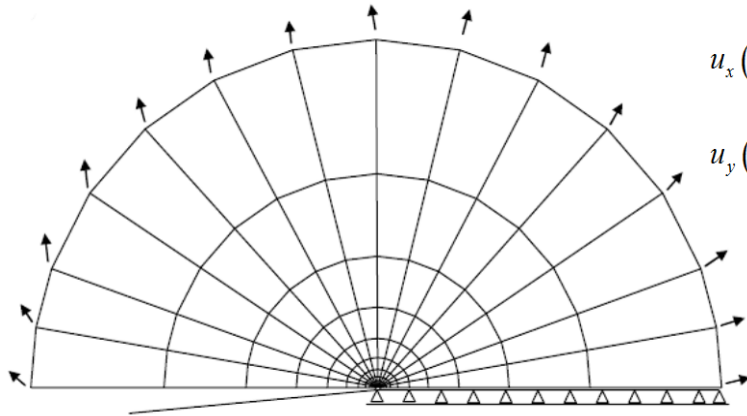
LEAD SIEGMUND

Creep-Fatigue Crack Growth Model Equations

<p><i>Damage-free traction-separation law:</i></p> $T_n = \sigma_{\max,0} e^{\left(\frac{\Delta_n}{\delta_0}\right)} \exp\left(-\frac{\Delta_n}{\delta_0}\right)$	
<p><i>Damage-free cohesive energy</i> $\phi_0 = \sigma_{\max,0} \delta_0 e$</p>	
<p><i>Fatigue damage increment</i></p> $\Delta D_F = \max\left\{0, \frac{ \dot{\Delta}_n }{\delta_\Sigma} \left[\frac{T_n}{\sigma_{\max}} - \frac{\sigma_f}{\sigma_{\max,0}} \right] \langle \Delta_{n,acc} - \delta_0 \rangle\right\}$	<p><i>Time-related damage increment</i></p> $\dot{D}_{KR} = (1-D)^{-p} \left\langle \frac{\bar{T} - T_C}{C} \right\rangle^q$
<p><i>Accumulated fatigue damage</i></p> ${}^n D_F = {}^{n-1} D_F + \Delta D_F$	<p><i>Accumulated time-related damage</i></p> ${}^n D_{KR} = {}^{n-1} D_{KR} + \dot{D}_{KR} \Delta t$
<p>Total damage $D = D_F + D_{KR}$</p> <p>Material fracture takes place when $D = 1$.</p>	
<p><i>Current cohesive strength</i></p> $\sigma_{\max} = \sigma_{\max,0} (1-D)$	
<p><i>Unloading/reloading condition:</i></p> $T_n = T_{n,\max} + \left[\frac{T_{n,\max}}{\Delta_{n,\max}} \right] (\Delta_n - \Delta_{n,\max})$	
<p><i>Traction-overclosure treatment:</i></p> $T_n = k_{\text{penalty}} \cdot \sigma_{\max,0} e^{\left(\frac{\Delta_n}{\delta_0}\right)} \exp\left(-\frac{\Delta_n}{\delta_0}\right)$	

LEAD SIEGMUND

Creep-Fatigue Crack Growth Simulation Model



$$u_x(t) = K_I(t) \sqrt{\frac{r}{2\pi}} \frac{1+\nu}{E} (3-4\nu - \cos \theta) \cos \frac{\theta}{2}$$

$$u_y(t) = K_I(t) \sqrt{\frac{r}{2\pi}} \frac{1+\nu}{E} (3-4\nu - \cos \theta) \sin \frac{\theta}{2}$$

$$r = \sqrt{x^2 + y^2}, \theta = \tan^{-1}(y/x)$$

MBL	ICZM	Material IN718
$r_b/l_e = 10,000$	$\delta_0 = 0.4 \times \min l_e$	$E = 165 \text{ GPa}$
$L/l_e = 110$	$\sigma_{\max,0} = 4\sigma_Y$	$\nu = 0.297$
$\Delta G/\phi_0 = 0.4$	$\sigma_f/\sigma_{\max,0} = 0.25$	$\sigma_0 = 779 \text{ MPa}$
	$\delta_\Sigma/\delta_0 = 4$	$\phi_0 = 62 \text{ kJ/m}^2$
	$p = 6, q = 3$	$b = 0.25 \text{ nm}$
	$C = 6000 \text{ MPa s}^{(1/3)}$	$\Lambda = 5000b$
	$T_C = 200 \text{ MPa}$	$m = 7$
		$\bar{\epsilon}_0 = 0.005 \text{ s}^{-1}$

Computations are consider a simplified strain gradient continuum model (no transient effects)

LEAD SIEGMUND

Creep-Fatigue Crack Growth Simulation Result



Creep-fatigue crack growth emerges as a complex interaction of creep & stress relaxation in the bulk together with cyclic & time dependent damage

LEAD SIEGMUND

Computational Mechanics

Implemented a strain gradient, unified viscoplastic constitutive theory needed for the description of the deformation response of IN718

Demonstrate the model in structures (disk) and for cracks

Creep-fatigue crack growth emerges from the competition of viscoplasticity (augmented by strain gradients), cycle-dependent and time-dependent damage

CONCLUSION

Creep-fatigue crack growth interaction emerges as the interaction and competition from multiple sources:

- Viscoplasticity and the gradient dependence of plasticity**
- Cycle dependent damage accumulation**
- Time dependent damage accumulation**

At high frequency or slow time-dependent damage (vacuum), cyclic damage dominates leading to transgranular failure

At low frequency or fast time-dependent damage (oxygen), time damage dominates leading to intergranular failure

Strain gradients play a significant role

Computational models available for predictions

CONV and AM both appear to exhibit similar deformation characteristic but the crack growth rate in the AM case is higher and the threshold is lower

CONTRIBUTION

Fundamentals

Creep-fatigue crack growth predictions accounting for fundamental mechanics

Turbines

NDE finds cracks → Diagnostics

Mechanics predicts how crack growth → Intelligence

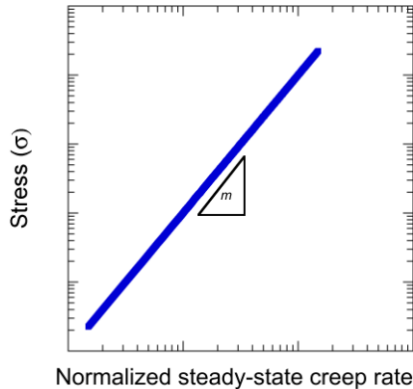
Reduce maintenance intervals

Realize digital twin with physics based engines

BACKUP SLIDES

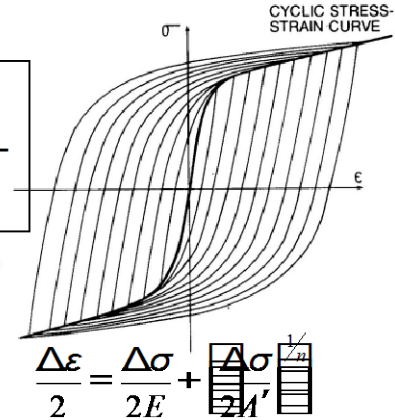
OVERVIEW: ORIGINAL PLAN

Research on Constitutive Parameters

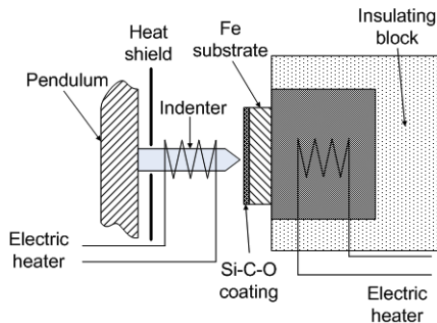


Uniaxial Creep at 650°C @ multiple stress levels

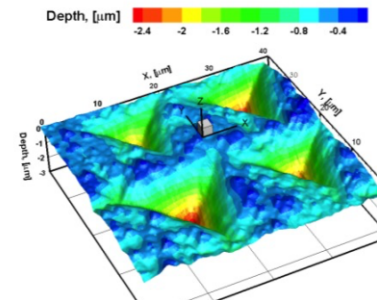
Tensile cyclic stress-strain at 650°C



Experimentally determined parameter	Symbol	Experiment
Reference stress	A'	Cyclic tensile tests
Cyclic strain hardening exponent	n	Cyclic tensile tests
Strain rate exponent	m	Uniaxial creep & Nanoindentation
Reference strain rate	$\dot{\epsilon}_0$	Uniaxial creep & Nanoindentation
Characteristic length scale	l	Nanoindentation
Dislocation-strain softening	ρ_i	Nanoindentation post creep

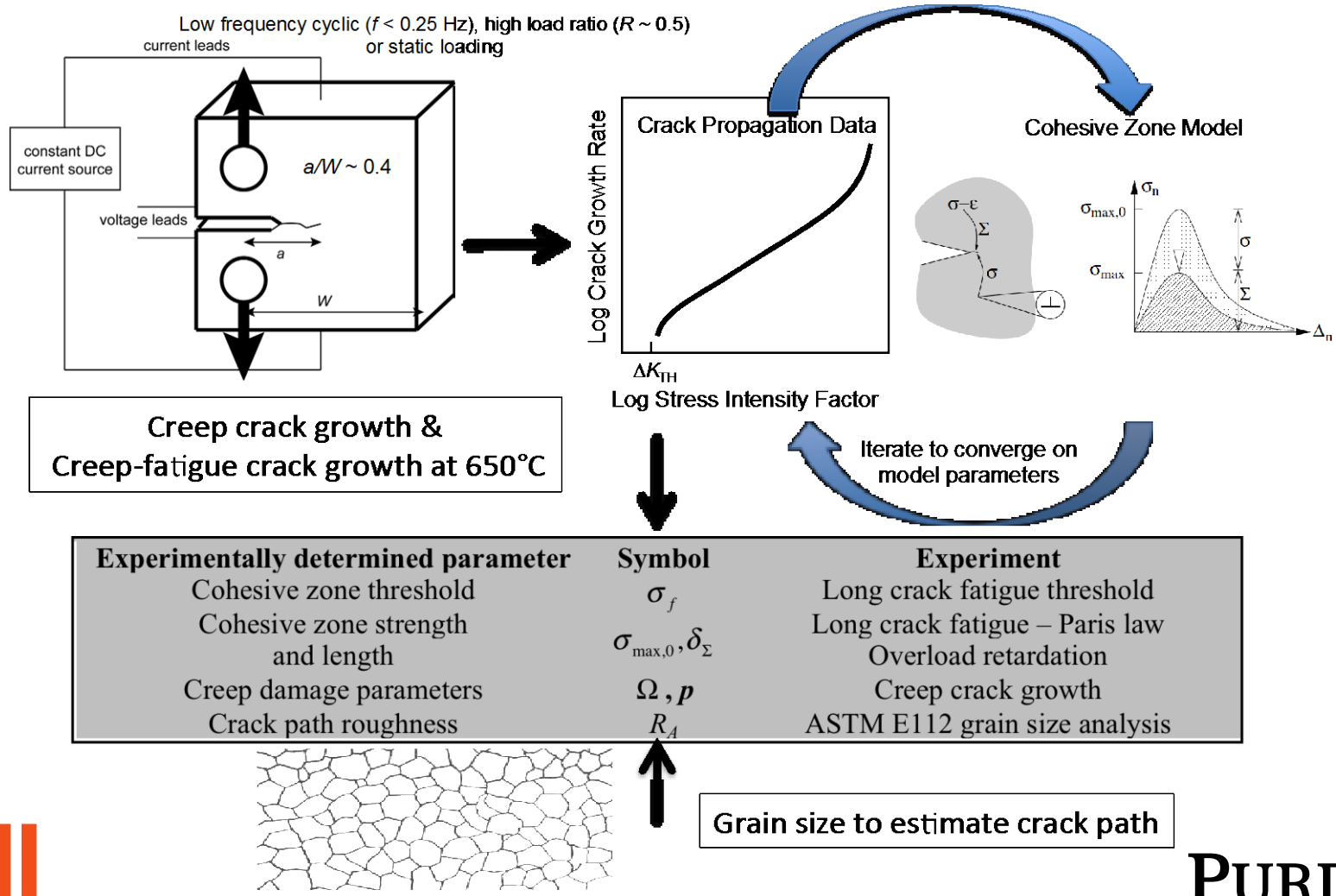


Nano-indentation at 650°C



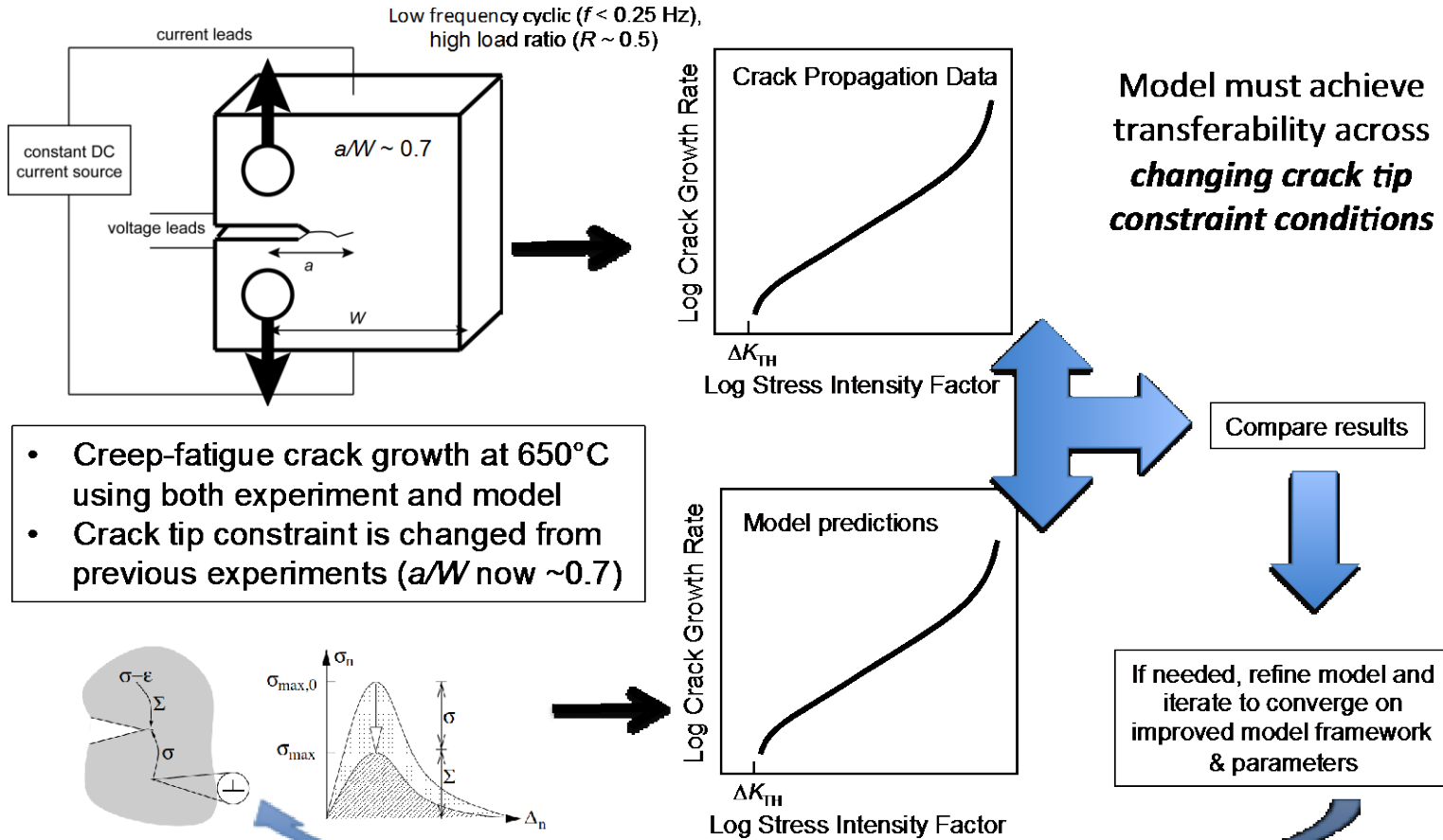
OVERVIEW: ORIGINAL PLAN

Research on Crack Propagation Models



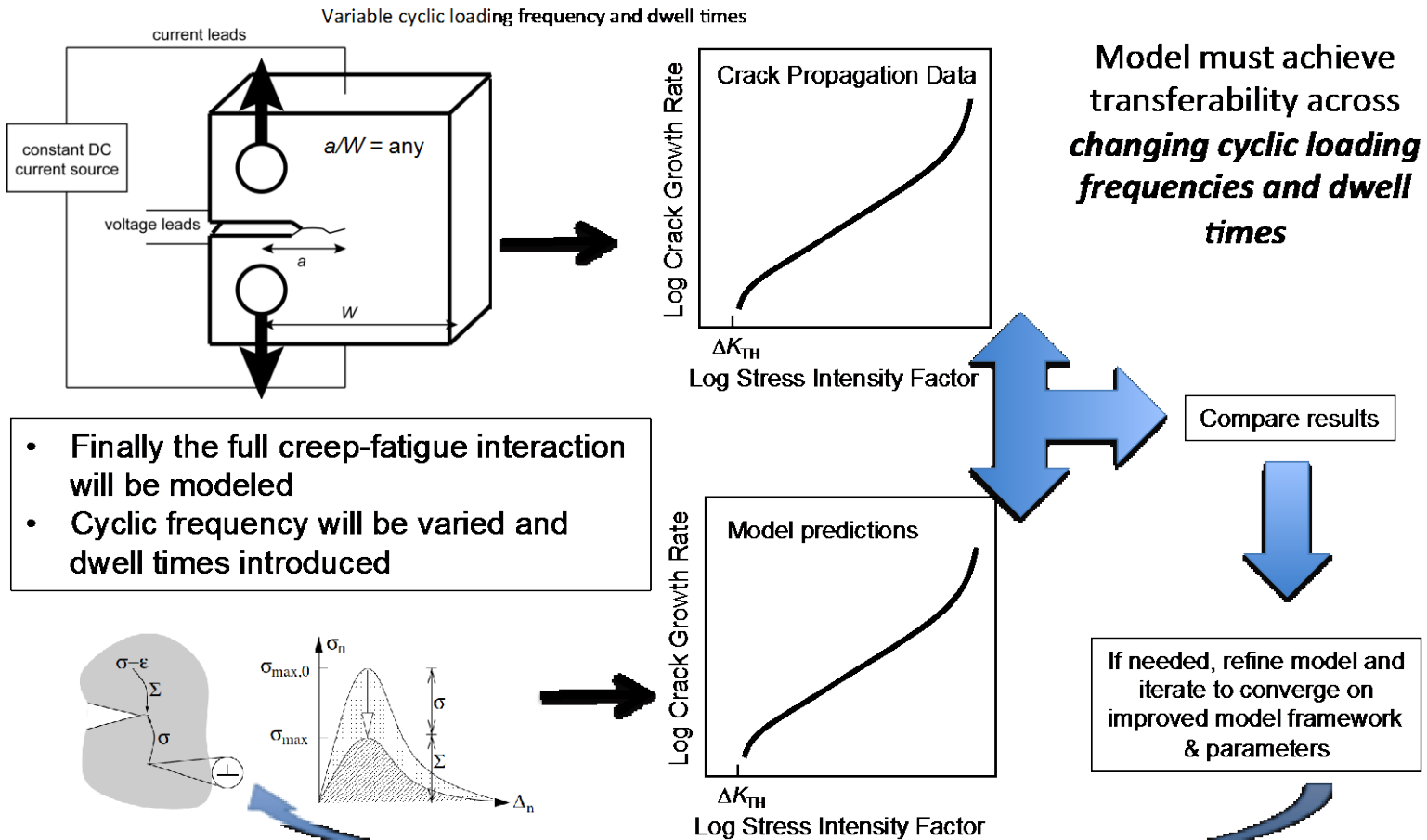
OVERVIEW: ORIGINAL PLAN

Initial Validation & Model Refinement



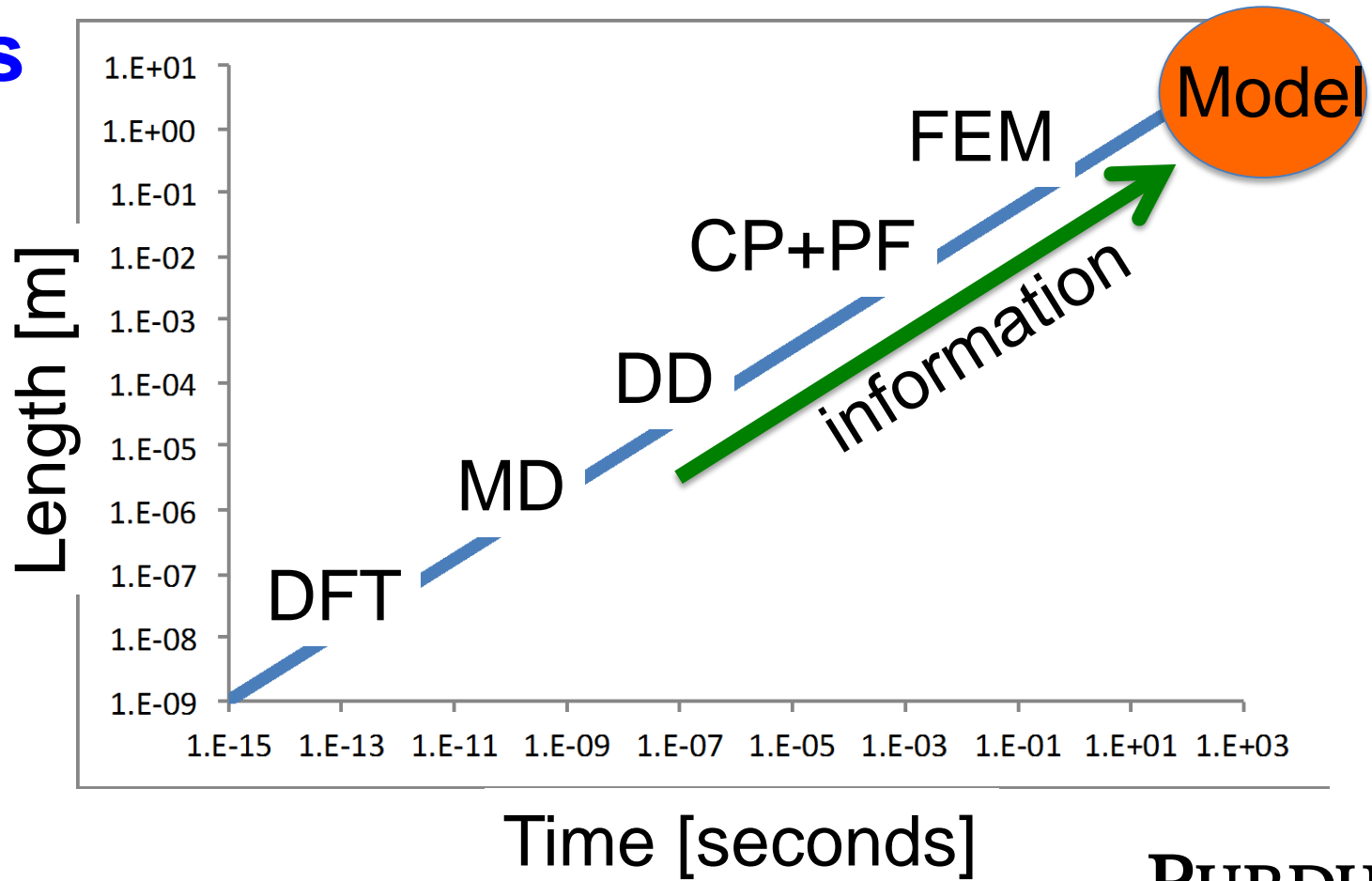
OVERVIEW: ORIGINAL PLAN

Final Validation & Model Refinement



OVERVIEW: LENGTH AND TIME

Small Scales and Long Times can only be addressed with advanced continuum models



2015: LEAD KRUZIC

Material Acquisition and Collaboration

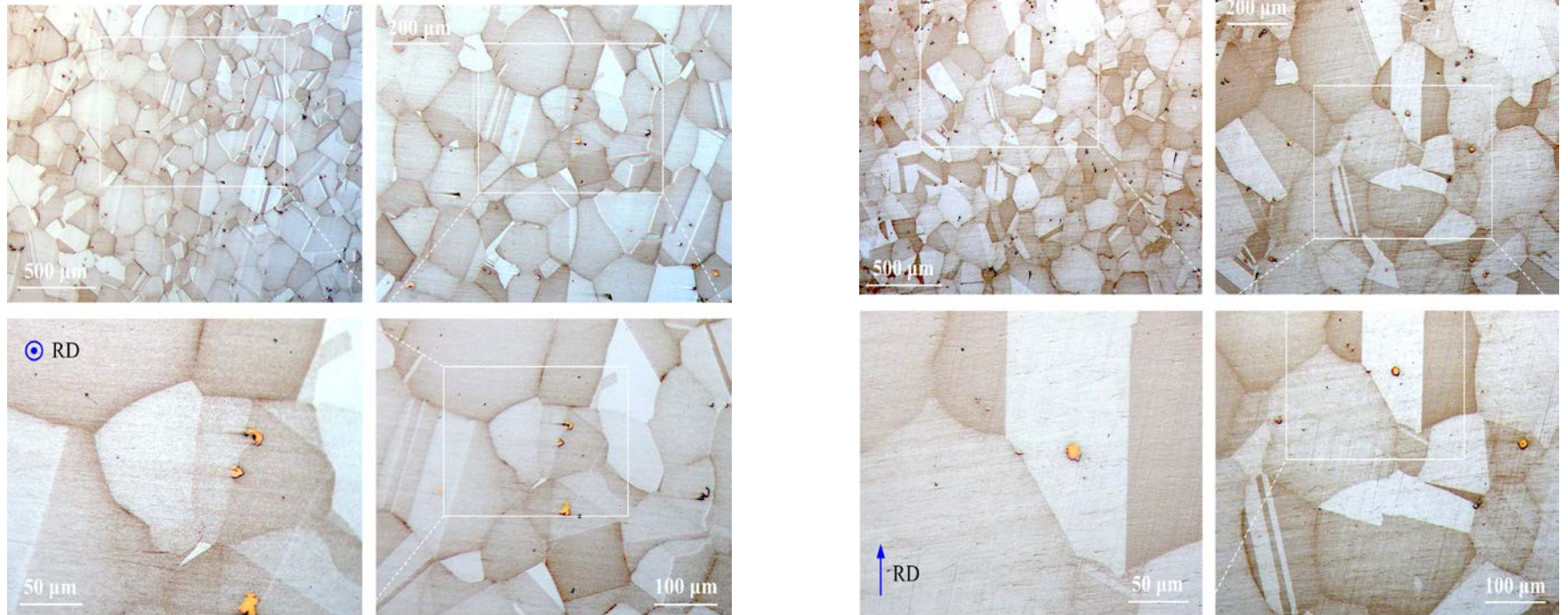
- **IN 718**
- **Provided by Jeff Hawk, NETL Albany**
- **Processing (at NETL)**

Step forging and squaring (from round slab $D=8.5''$ to plate $t=1.25''$); Hot rolling into a plate $t=0.616''$; solution annealed. Received a plate roughly $27'' \times 5 \frac{5}{8}'' \times 0.616''$.
- **Processing (at OSU)**

Solution annealed at 982°C , 1hr, air cooled Hardened by holding at 718°C for 8hrs, then furnace cooled to 621°C and held for 10 hrs, then air cooled.

2015

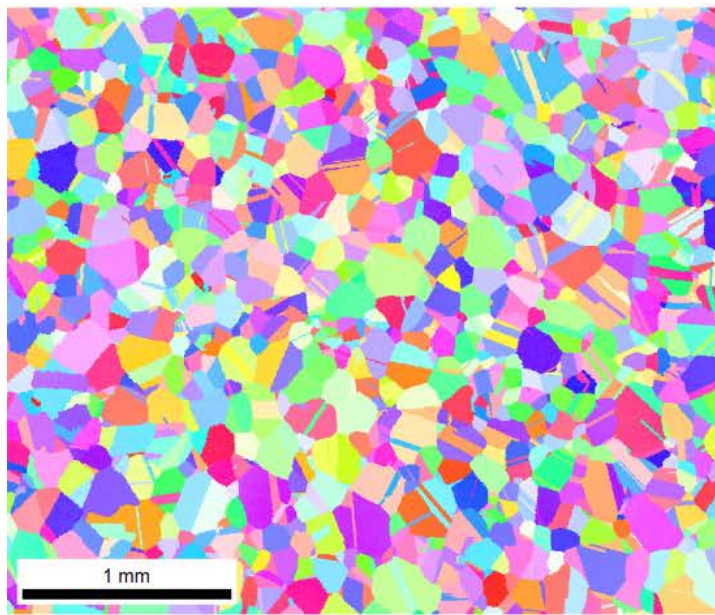
Optical Microstructure Characterization



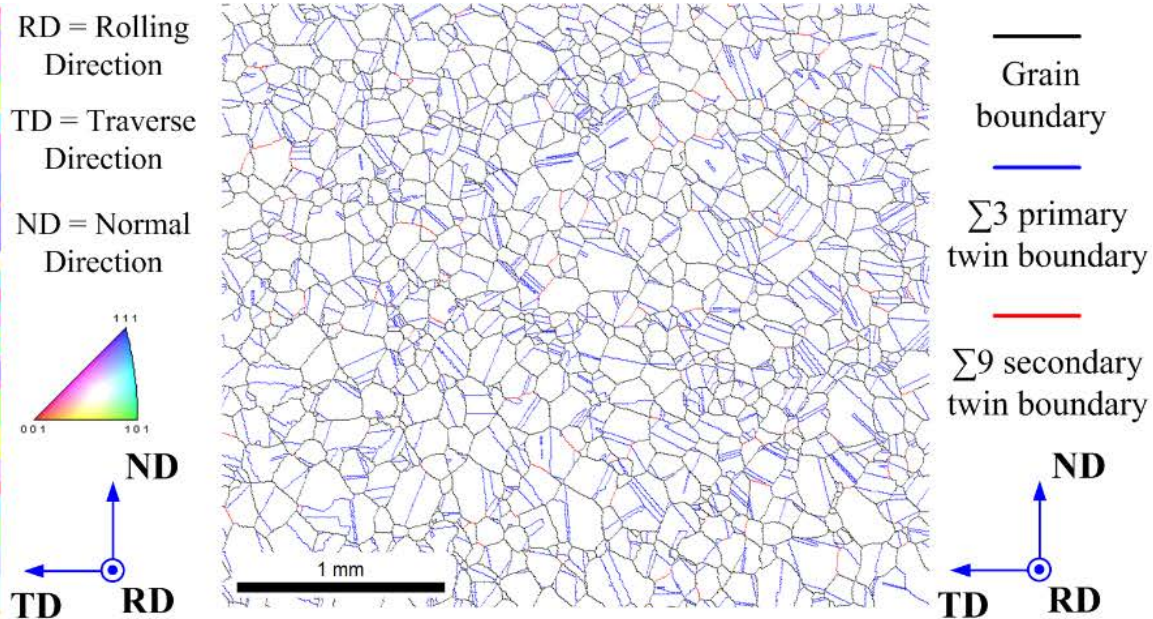
Uniform and equiaxed microstructure

2015

EBSD on Transverse Section



(a) Crystal orientation map

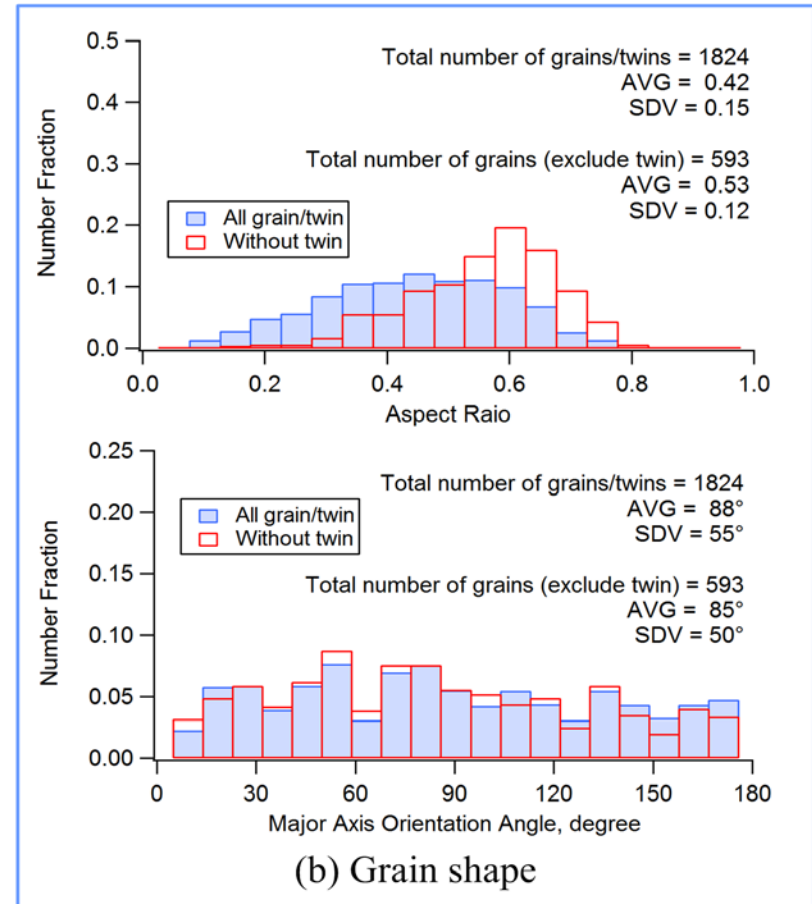
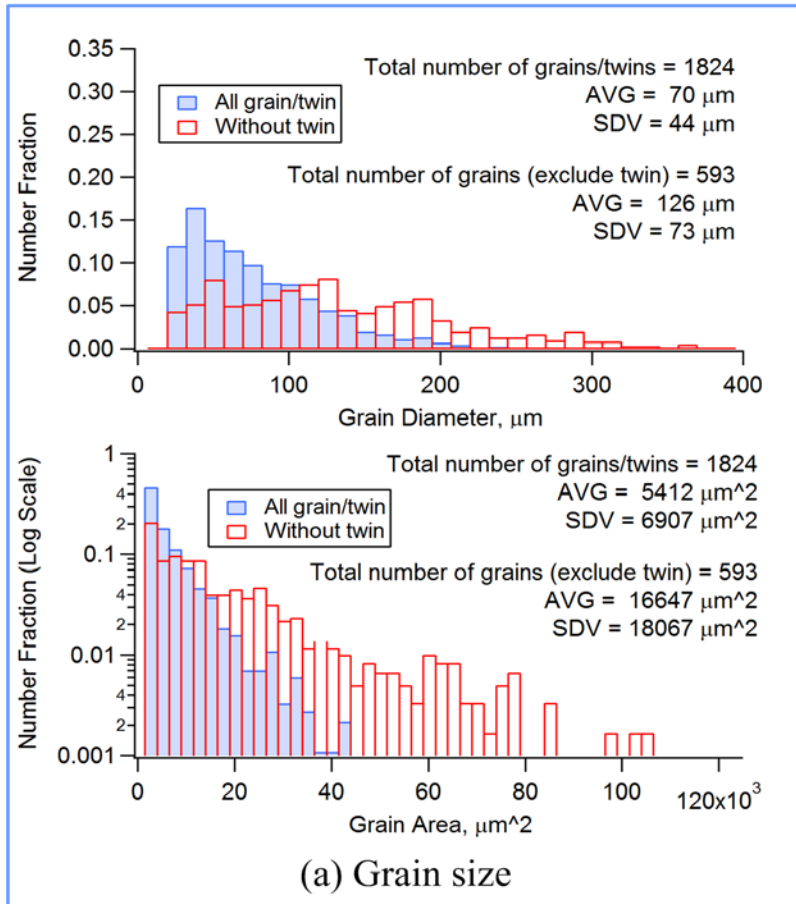


(b) Grain/twin boundary map

Highly twinned

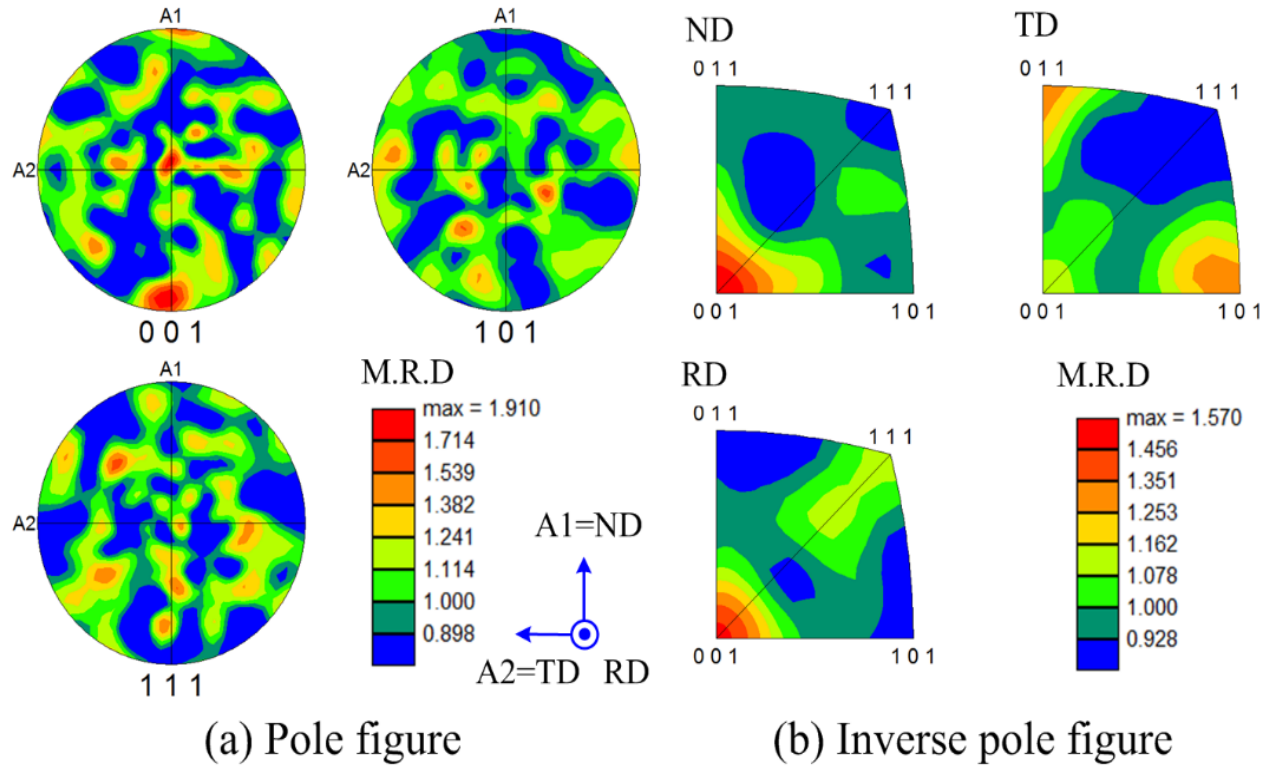
Most twins as $\Sigma 3$ (from recrystallization)

Grains & Twins: Grain Size and Orientation



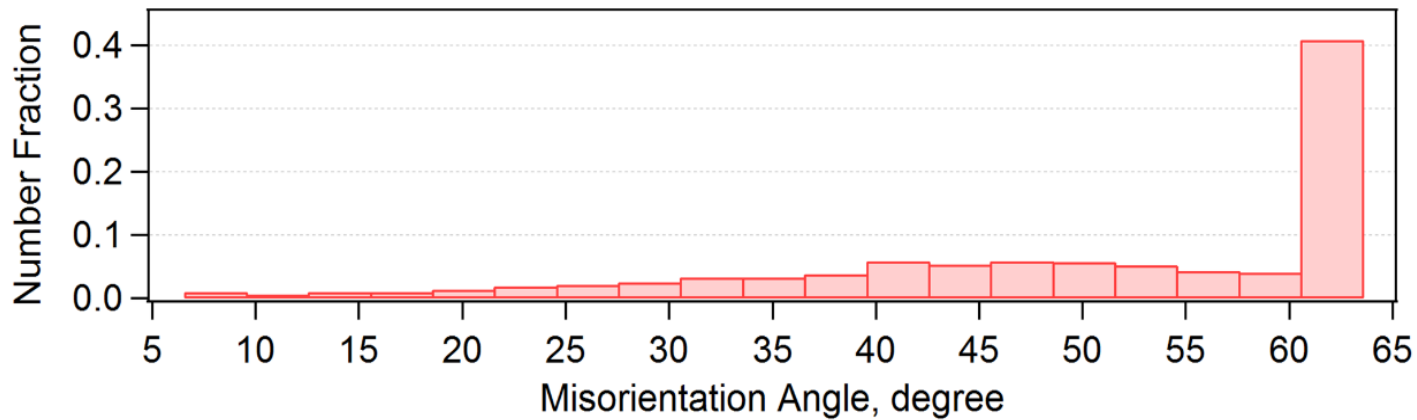
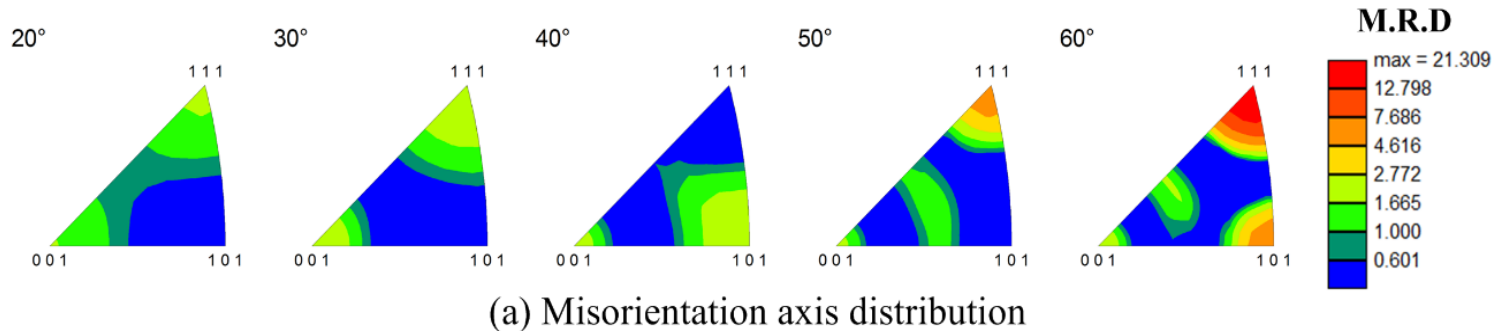
Analysis with and without twins

Texture



Only weak initial texture, remnants of a cube (100)[001] and even weaker fiber <111> texture exist

Grain and Twin Boundaries

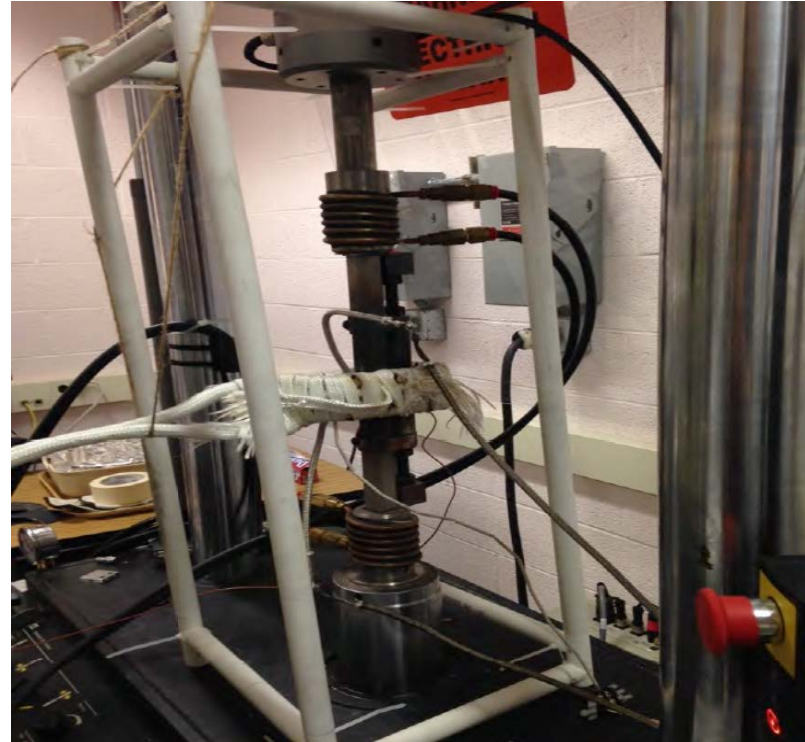
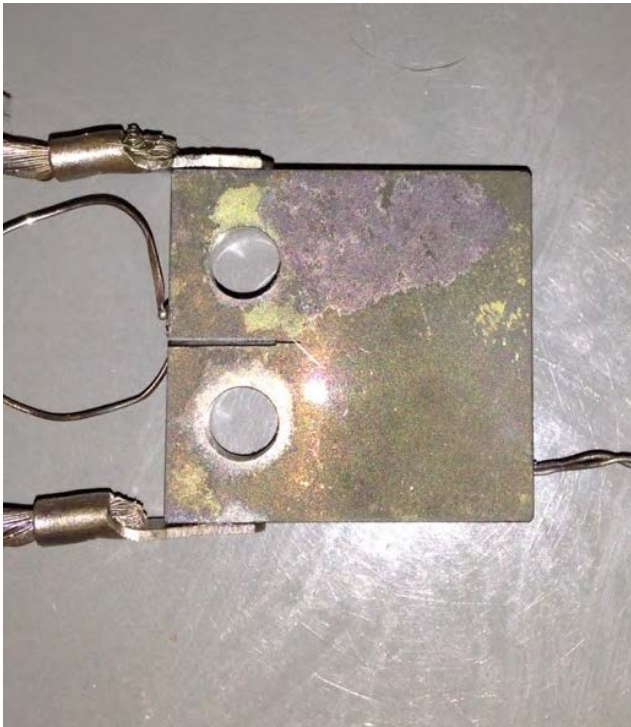


(b) Misorientation angle distribution

Strongly influenced by S3 twins

2015

Crack Growth: Experimental Set Up



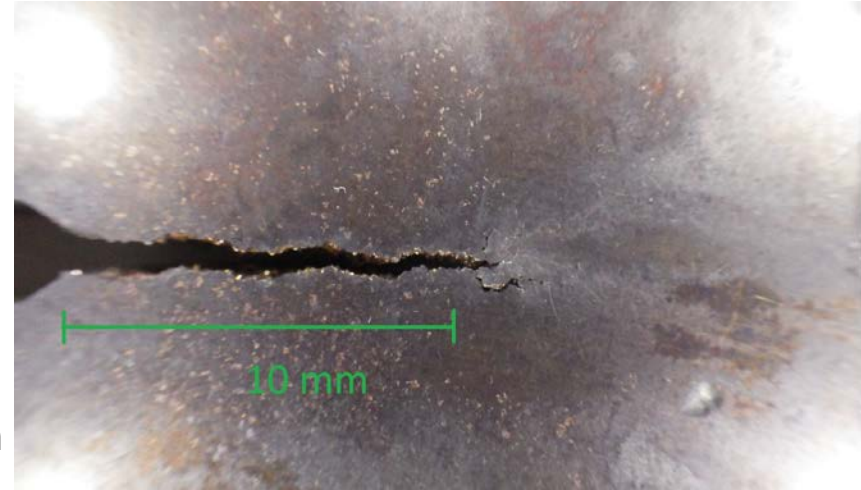
HT Experiments on CT specimens with potential drop measurements

2015

Crack Growth: Initial Experiments

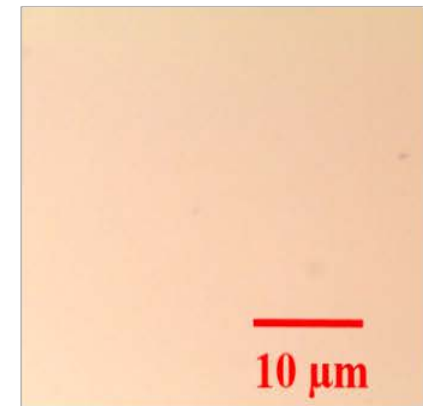
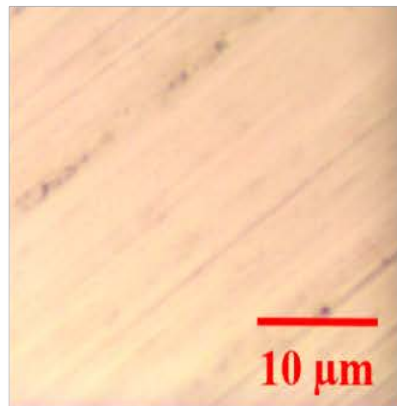
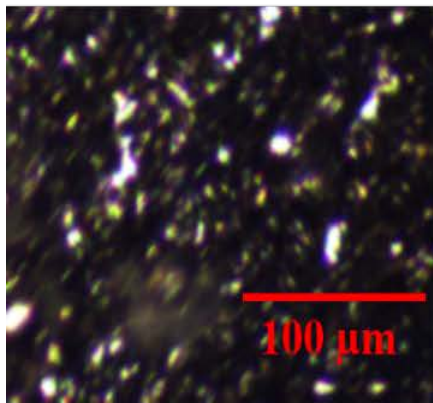
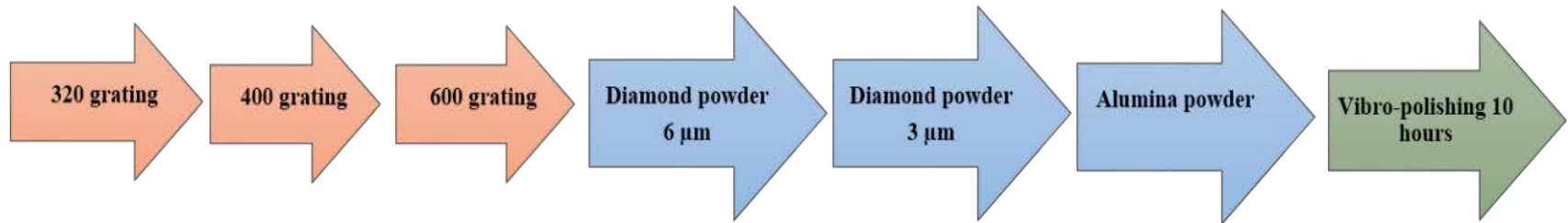
Test parameters:

- Compact tension C(T) sample
- Constant force range, ΔP
- Load ratio, $P_{\min}/P_{\max} = R = 0.5$
- 0.1 Hz triangle waveform
- $T = 650^{\circ}\text{C}$ in air
- Crack was grown from $a = 6.5 - 16.7$ mm



2015

HT Nanoindentation: Specimen preparation



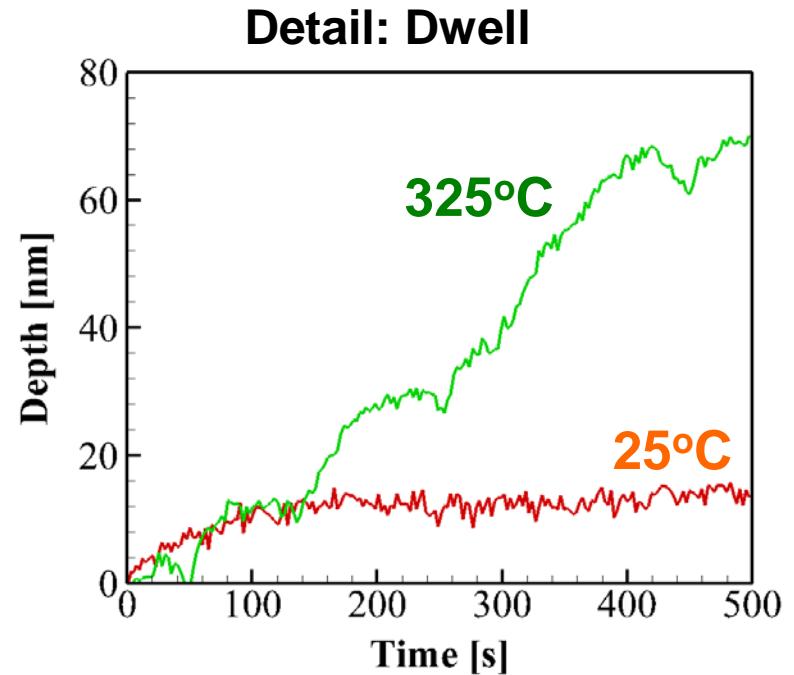
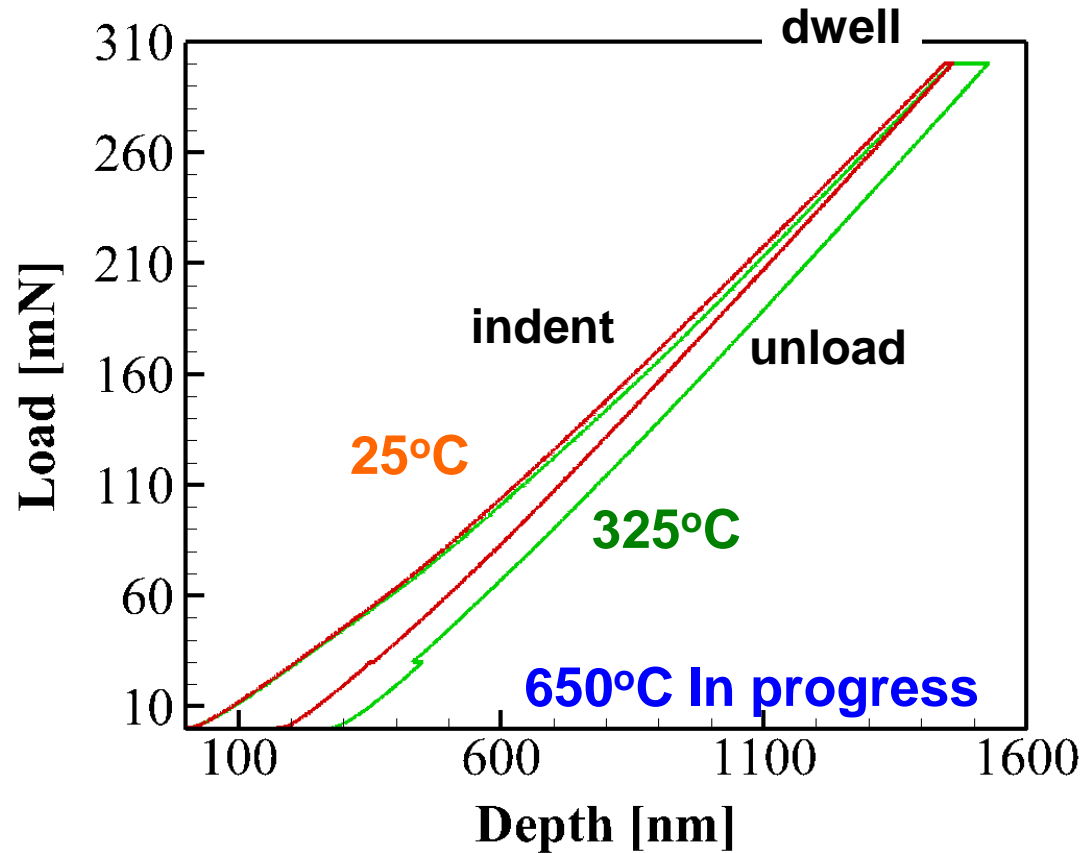
HT Nanoindentation: Experimental plan

Through change in indent depth the ratio of **viscoplast. strain & viscoplast. strain gradient** is altered → obtain the relevant length scale

Load (mN)	25 °C (no. of points)	350 °C (no. of points)	650 °C (no. of points)	Post oxidation (no. of points)	Dwell time (s)
50	10	10	10	10	500
100	10	10	10	10	500
200	10	10	10	10	500
300	10	10	10	10	500
400	10	10	10	10	500

2015

HT Nanoindentation: 1st data on IN 718



Current Status

- Calibrate indentation system to account for machine compliance at high temperature (ceramic)
- Currently, waiting for indenter tip to be provided by manufacturer. Delayed due to end of year closures and budget allocations
- Expect indenter tip back at Purdue with a short time

Constitutive Models: Flow Stress

$$\sigma_{\text{flow}} = \sigma_0 + M \alpha \mu b \sqrt{\rho_S + \rho_G} = \sigma_0 \left(1 + \frac{\sqrt{3} \alpha \mu b}{\sigma_0} \sqrt{\frac{\sqrt{3} \bar{\epsilon}^{vp}}{b \Lambda} + \frac{\bar{\eta}}{b}} \right)$$

$$\Delta \dot{\bar{\epsilon}}^{vp} = g(\boldsymbol{\sigma}, \mathbf{q}) \quad \mathbf{q}: \text{state variable vector}$$

$$\Delta \bar{\epsilon}^{vp} = \Delta t \dot{\bar{\epsilon}}^{vp} = \Delta t \cdot g(\boldsymbol{\sigma}, \mathbf{q}) = \Delta t \dot{\bar{\epsilon}}_0 \left(\frac{\bar{\sigma}}{\sigma_{\text{flow}}} \right)^m$$

$$\left(\frac{J}{2\sigma_0} / \Lambda \right), (b / \Lambda), \left(\frac{j}{2\sigma_y} / \dot{\bar{\epsilon}}_0 \Lambda \right)$$

Computational Implementation

$$\dot{\epsilon}_{ij} = \frac{\dot{\sigma}_{ij}}{9K} \delta_{ij} + \frac{\dot{s}_{ij}}{2\mu} + \frac{3\dot{\bar{\epsilon}}^{vp}}{2\bar{\sigma}} \dot{s}_{ij} = \frac{\dot{\sigma}_{ij}}{9K} \delta_{ij} + \frac{\dot{s}_{ij}}{2\mu} + \frac{3\dot{\bar{\epsilon}}_0}{2\bar{\sigma}} \left(\frac{\bar{\sigma}}{\sigma_0 \left(1 + \frac{\sqrt{3}\alpha\mu b}{\sigma_0} \sqrt{\frac{\sqrt{3}\bar{\epsilon}^{vp}}{b\Lambda} + \frac{\bar{\eta}}{b}} \right)} \right)^m \dot{s}_{ij}$$

$$\dot{\sigma}_{ij} = K\dot{\epsilon}_{ij}\delta_{ij} + 2\mu \left\{ \dot{\epsilon}'_{ij} - \frac{3\dot{\bar{\epsilon}}_0}{2\bar{\sigma}} \left[\frac{\bar{\sigma}}{\sigma_0 \left(1 + \frac{\sqrt{3}\alpha\mu b}{\sigma_0} \sqrt{\frac{\sqrt{3}\bar{\epsilon}^{vp}}{b\Lambda} + \frac{\bar{\eta}}{b}} \right)} \right]^m \dot{s}_{ij} \right\}$$

Computational Implementation

Euler implicit scheme + Newton-Raphson iteration

- Nonlinear equations

$$f_1(\Delta\bar{\epsilon}^{vp}, \bar{\sigma}) = \Delta\bar{\epsilon}^{vp} - \Delta t \dot{\bar{\epsilon}}_0 \left(\frac{\bar{\sigma}}{\sigma_{\text{flow}}} \right)^m = 0$$

$$f_2(\Delta\bar{\epsilon}^{vp}, \bar{\sigma}) = 3\mu(\bar{\epsilon}^* - \Delta\bar{\epsilon}^{vp}) - \bar{\sigma} = 0$$

- Trial state

$$\boldsymbol{\epsilon}_{n+1}^{trial} = \boldsymbol{\epsilon}_n^{el} + \Delta\boldsymbol{\epsilon}; \quad \bar{\epsilon}^* = \sqrt{\frac{2}{3} \boldsymbol{\epsilon}_{n+1}^{trial} : \boldsymbol{\epsilon}_{n+1}^{trial}}$$

Computational Implementation

- Iteration

$$\begin{Bmatrix} \Delta \bar{\epsilon}^{vp} \\ \bar{\sigma} \end{Bmatrix}_{n+1} = \begin{Bmatrix} \Delta \bar{\epsilon}^{vp} \\ \bar{\sigma} \end{Bmatrix}_n - \mathbf{J}_n^{-1} \begin{Bmatrix} f_1(\Delta \bar{\epsilon}^{vp}, \bar{\sigma}) \\ f_2(\Delta \bar{\epsilon}^{vp}, \bar{\sigma}) \end{Bmatrix}_n$$

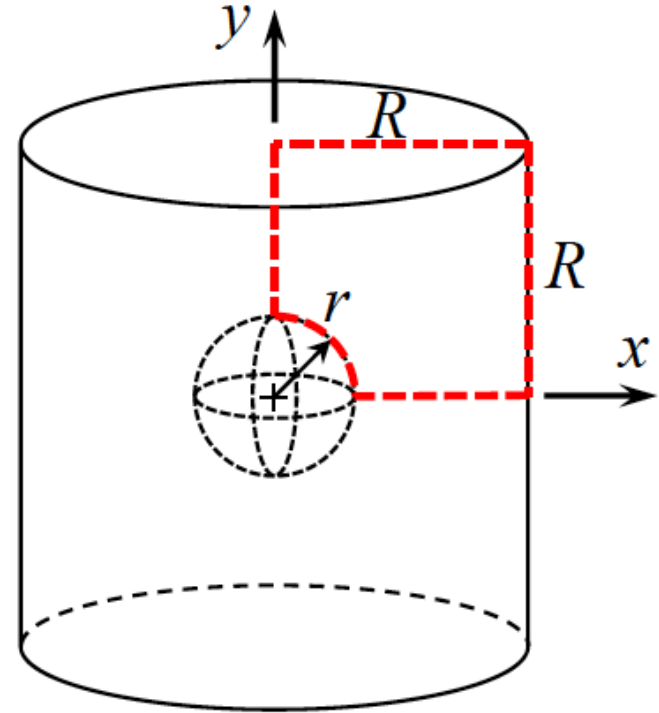
$$\mathbf{J}_n = \begin{bmatrix} \frac{\partial f_1}{\partial \Delta \bar{\epsilon}^{vp}} & \frac{\partial f_1}{\partial \bar{\sigma}} \\ \frac{\partial f_2}{\partial \Delta \bar{\epsilon}^{vp}} & \frac{\partial f_2}{\partial \bar{\sigma}} \end{bmatrix}_n$$

$$\bar{\epsilon}_{n+1}^{vp} = \bar{\epsilon}_n^{vp} + \Delta \bar{\epsilon}^{vp}$$

- Stress update follows a standard procedure upon convergence of the above iteration.

2015

Results: Creep Rupture

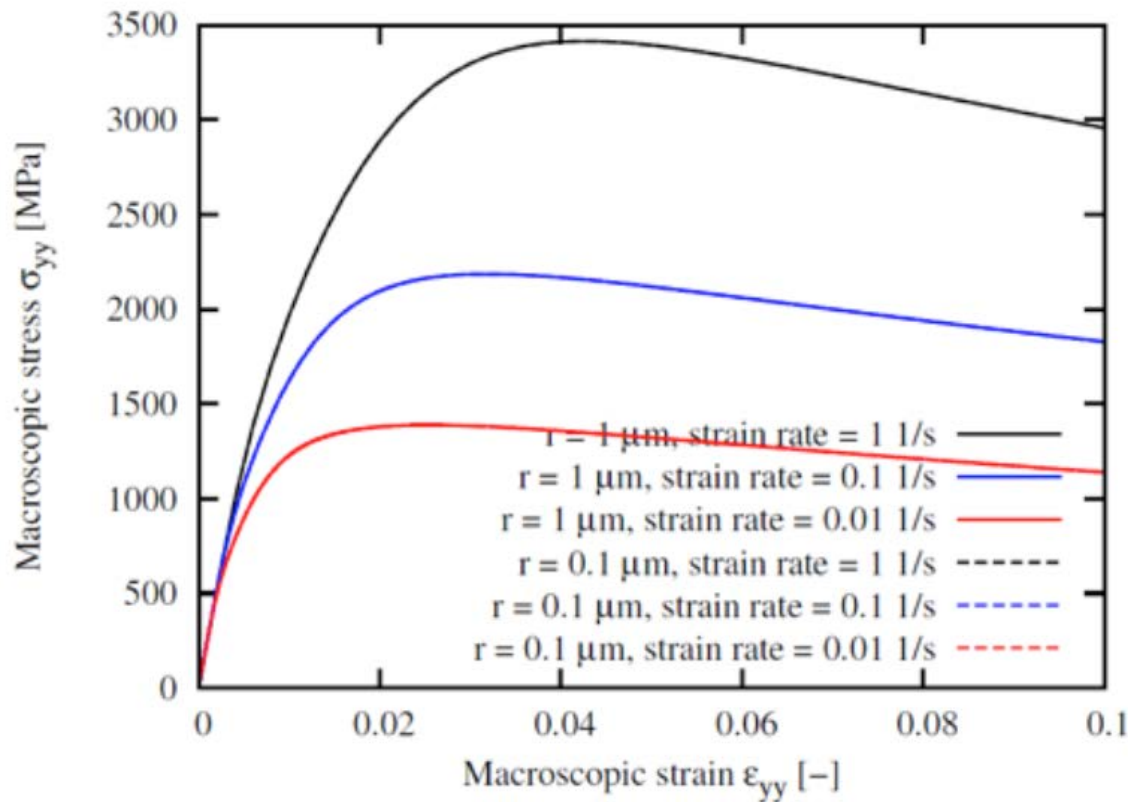


E (GPa)	ν	σ_{y0} (MPa)	$\dot{\epsilon}_0$ (s^{-1})	m	b (nm)
200	0.3	250	0.005	5	0.25

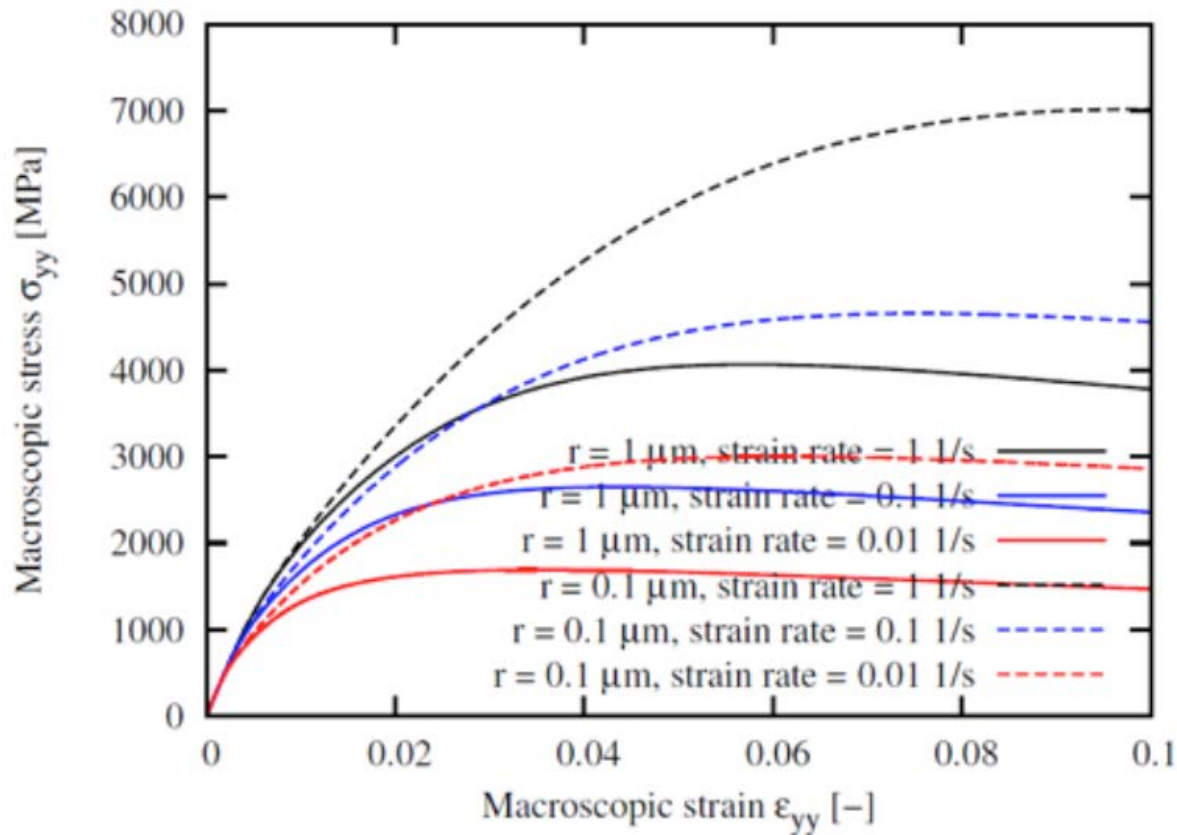
2015

Void Growth conventional plasticity

No size effect only rate effect



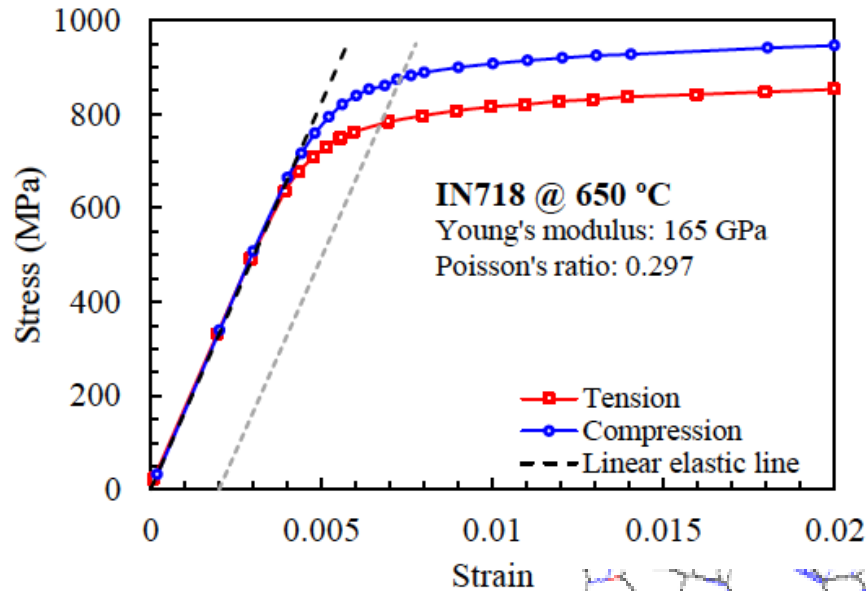
Void Growth with SGP: Void Size Effect combined with a rate effect



- Smaller voids lead to higher stresses
- Smaller voids are more sensitive to rate

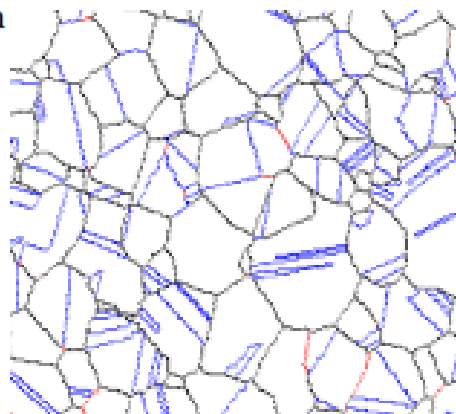
2015

Strength Differential Effect (Data by Lissenden et al)



$$SD = 2 \frac{|\sigma_C| - |\sigma_T|}{|\sigma_C| + |\sigma_T|} = 0.12$$

$$SR = \frac{|\sigma_T|}{|\sigma_C|} = 0.88$$



Strength Differential Effect: Yield Function

$$\Phi(s_1, s_2, s_3) = \left(|s_1| - k \cdot s_1 \right)^m + \left(|s_2| - k \cdot s_2 \right)^m + \left(|s_3| - k \cdot s_3 \right)^m$$

m, k

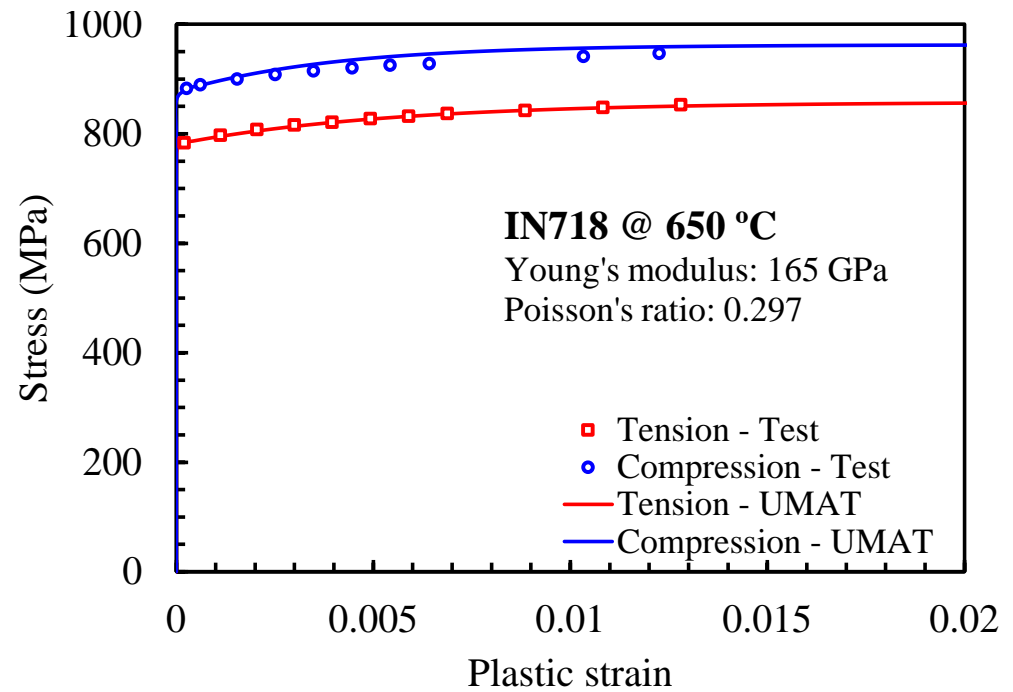
$m = 2, k = 0 \dots$ von Mises

$$k = \frac{1 - \left\{ \frac{2^m - 2 \cdot (\sigma_T / \sigma_C)^m}{(2 \cdot \sigma_T / \sigma_C)^m - 2} \right\}^{(1/m)}}{1 + \left\{ \frac{2^m - 2 \cdot (\sigma_T / \sigma_C)^m}{(2 \cdot \sigma_T / \sigma_C)^m - 2} \right\}^{(1/m)}}$$

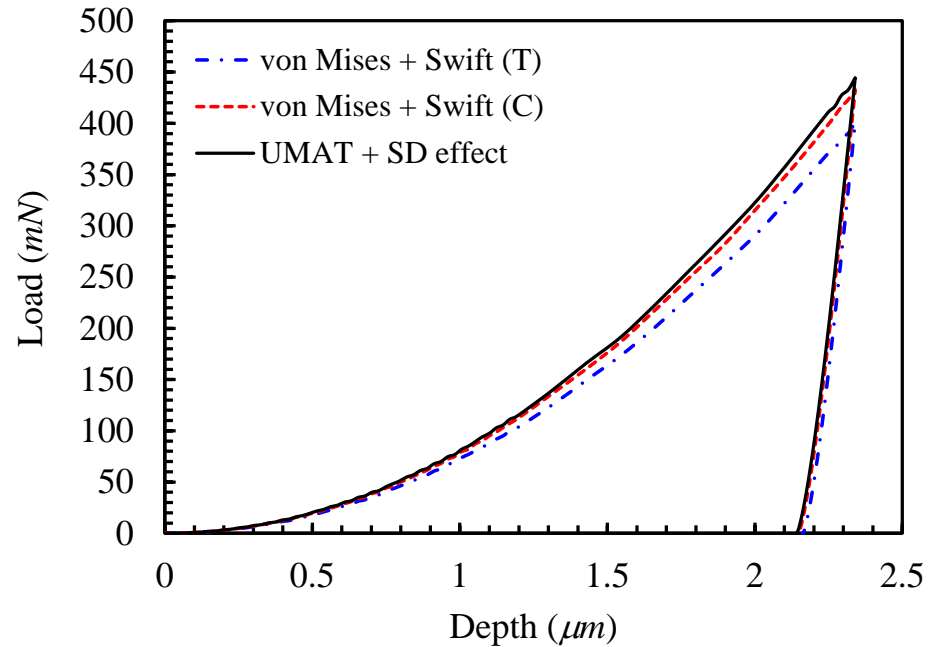
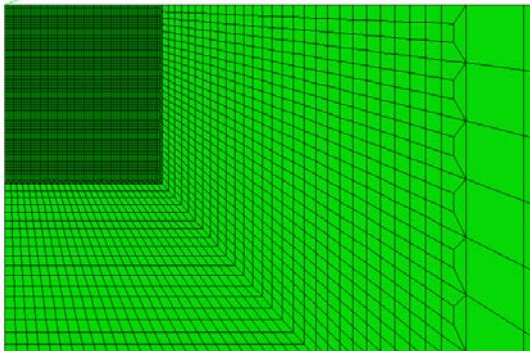
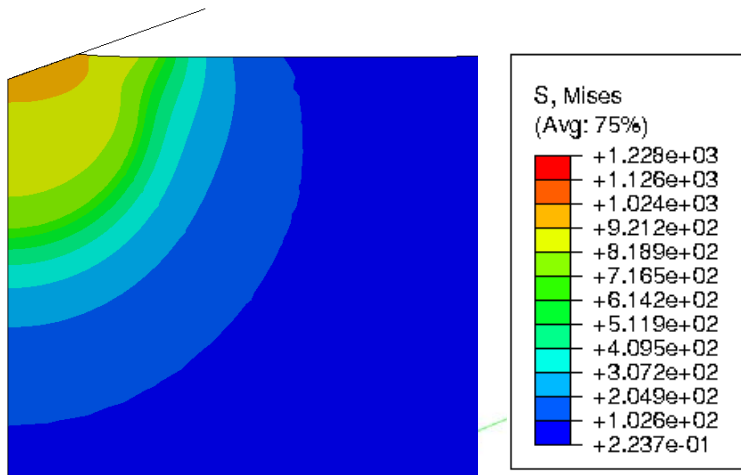
Strength Differential Effect: UMAT

E (GPa)	ν	σ_T (MPa)	σ_C (MPa)	K (MPa)	ϵ_0	n
165	0.297	779	876	1003	0.0013	0.038

$$\sigma = K \left(\epsilon_0 + \bar{\epsilon} \right)^n$$



Strength Differential & Indentation



Von Mises + Swift (T)	Von Mises + Swift (C)	UMAT w/ SD
1.0	1.09	1.12

Crack Growth: Cohesive Zone Models

$$T_n = \sigma_{\max,0} e^{\left(\frac{\Delta_n}{\delta_0}\right)} \exp\left(-\frac{\Delta_n}{\delta_0}\right)$$

$$\sigma_{\max} = \sigma_{\max,0} (1 - D_C)$$

$$\Delta D_C = \max \left\{ 0, \frac{|\dot{\Delta}_n|}{\delta_{\Sigma}} \left[\frac{T_n}{\sigma_{\max}} - \frac{\sigma_f}{\sigma_{\max,0}} \right] H(\Delta_{n,acc} - \delta_0) \right\}$$

$$\Delta_{n,acc} = \int_t |\dot{\Delta}_n| dt$$

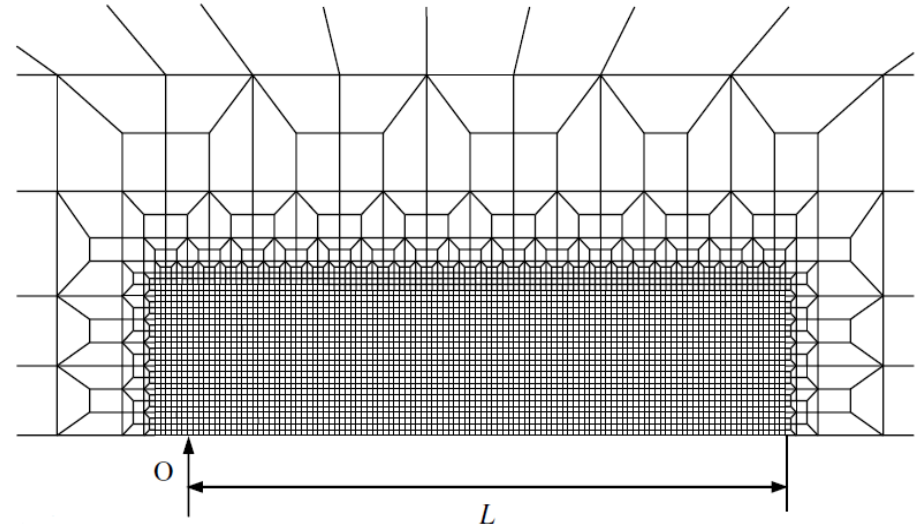
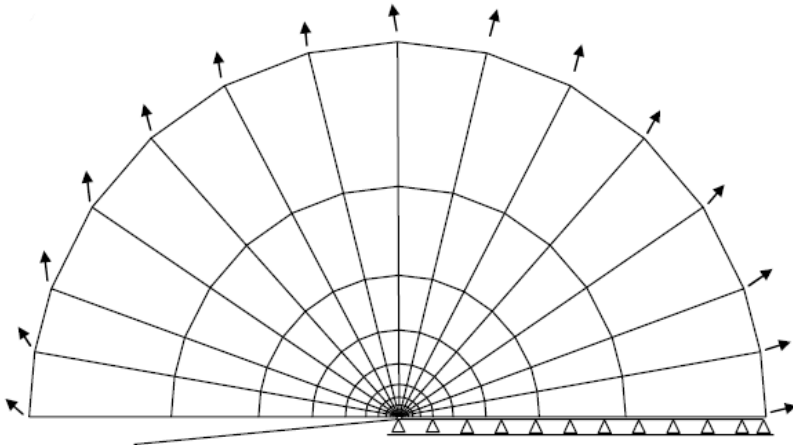
$$D_C = D_C + \Delta D_C$$

$$\left(\frac{J}{2\sigma_0} / \Lambda \right), (b / \Lambda), \left(\frac{j}{2\sigma_y} / \dot{\epsilon}_0 \Lambda \right), (\delta / \Lambda)$$

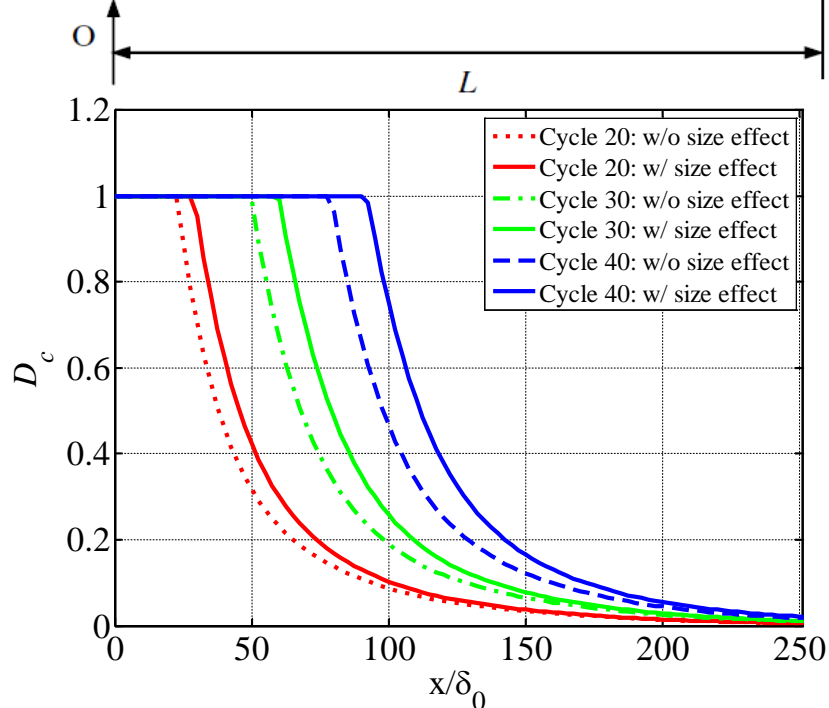
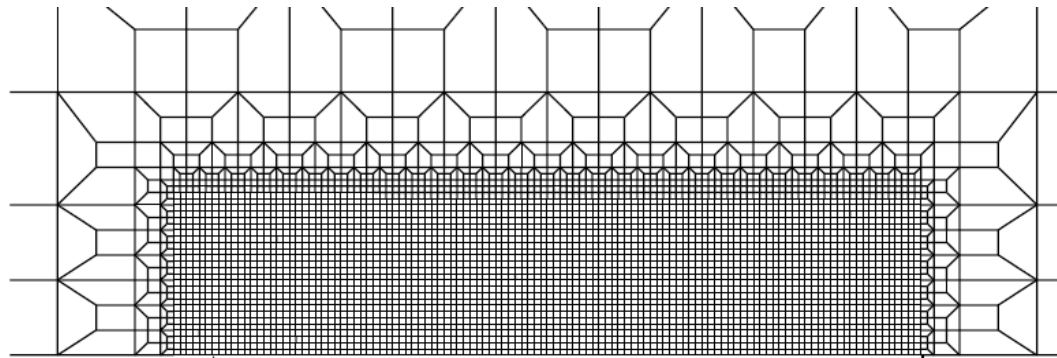
2015

Modified Boundary Layer Model

$$u_x(t) = K_I(t) \sqrt{\frac{r}{2\pi}} \frac{1+\nu}{E} (3-4\nu - \cos\theta) \cos\frac{\theta}{2}$$
$$u_y(t) = K_I(t) \sqrt{\frac{r}{2\pi}} \frac{1+\nu}{E} (3-4\nu - \cos\theta) \sin\frac{\theta}{2}$$
$$K(t) = \sqrt{\frac{EG(t)}{(1-\nu^2)}}$$

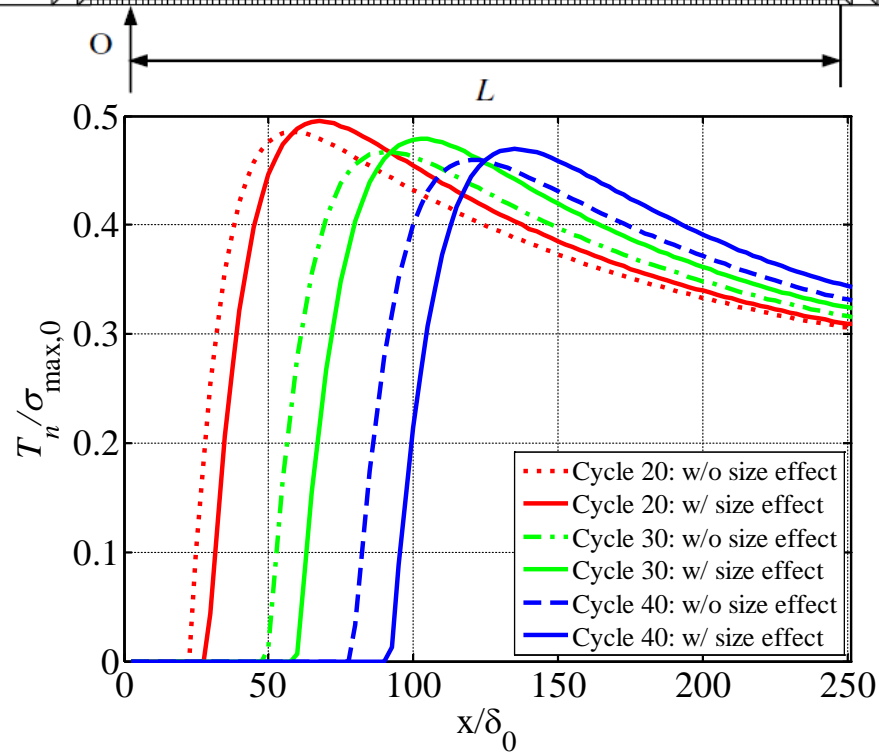
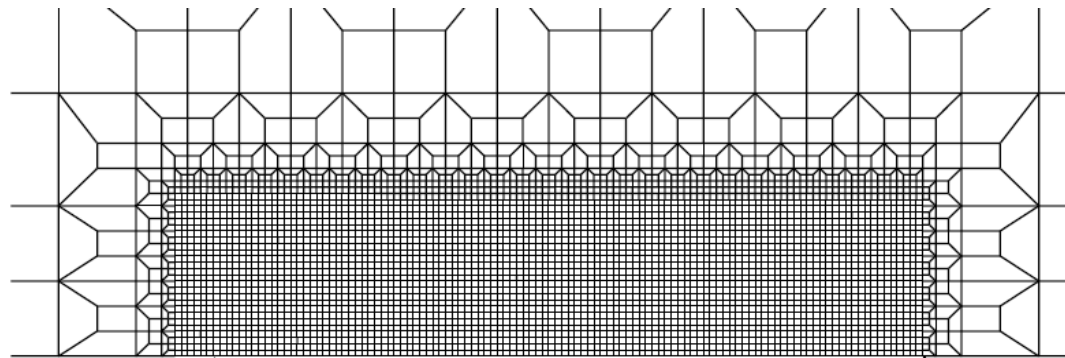


Strain Gradients and FCG



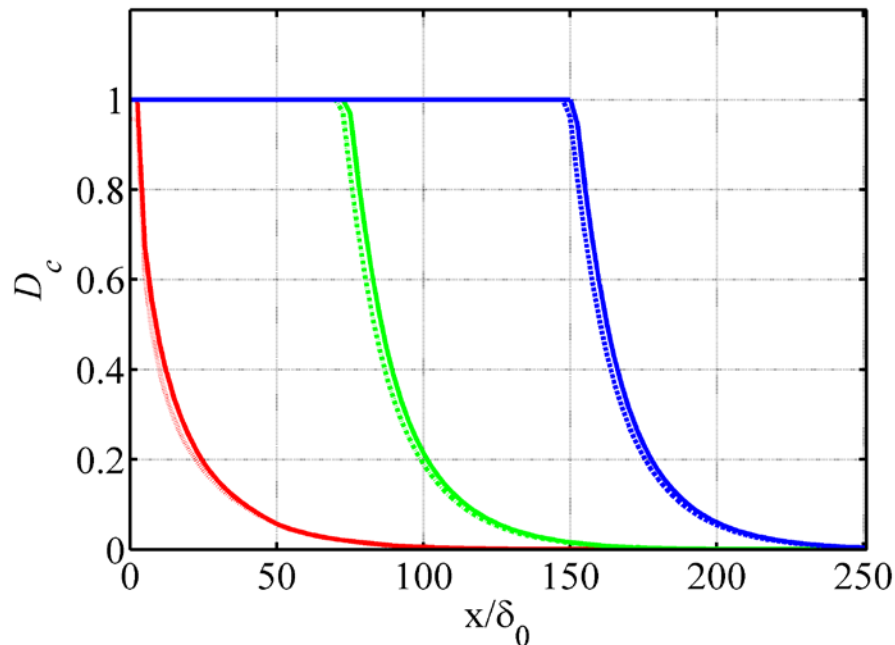
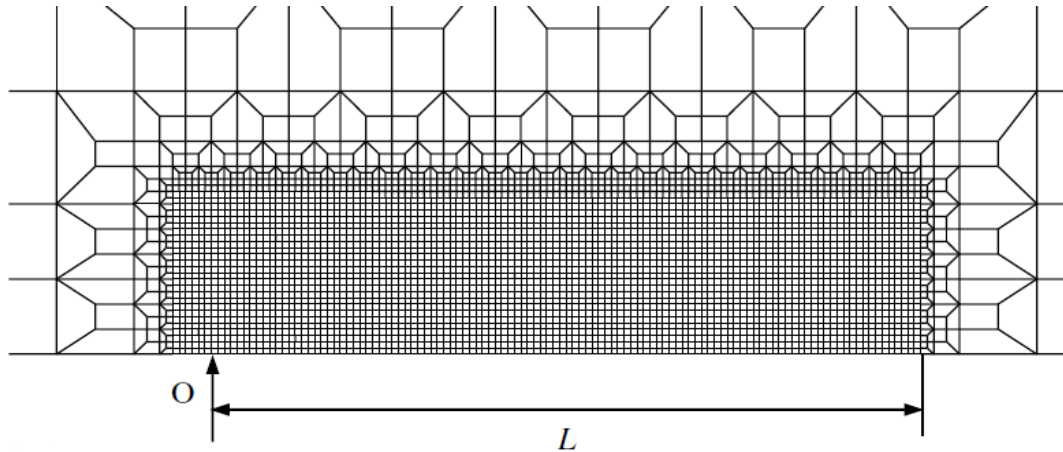
- FCG Rates with SGP are larger than without

Strain Gradients and FCG



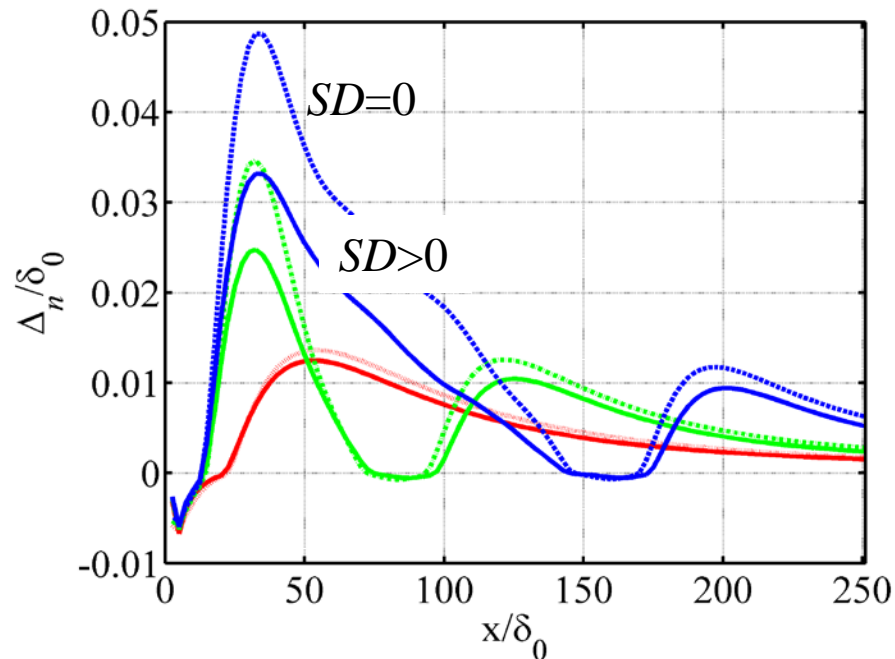
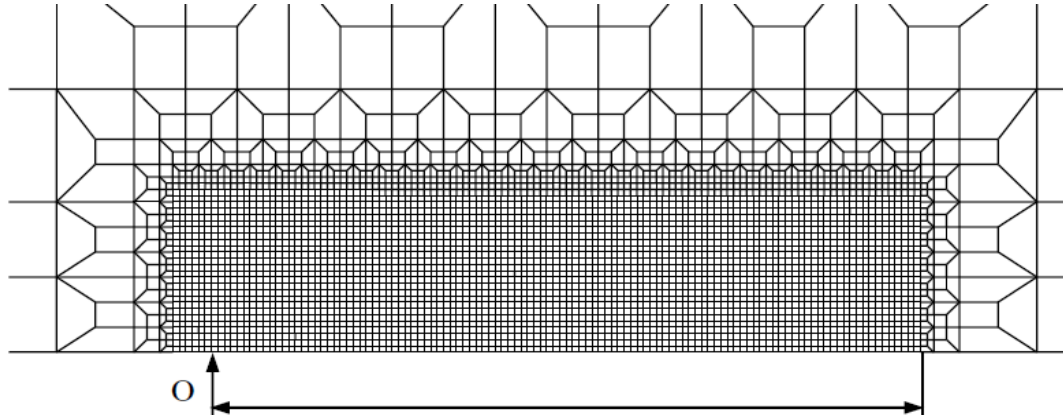
- Opening stresses with SGP are larger than without

Strength Differential and FCG



- FCG Rates appear as little affected by SD alone

Strength Differential and FCG



- Crack closure appear as affected by SD alone

2015 CONCLUSION

- **Procured and characterized materials (NETL Albany)**
- **Property measurements ongoing**
- **Computational mechanics: Advanced model implementation on several fronts**

- **Additional Potential Actions:**
 - **Establish a tentative collaboration to explore AM manufactured materials**
 - **Follow up with industry showed interest but no concrete action**
 - **Explore the use of methods in structural part (blisk)**